

國立交通大學

電信工程學系碩士班
碩士論文

新穎正交分頻多重存取系統之測距方式
A Novel Ranging Method for OFDMA Systems

研究生：林坤昌

指導教授：蘇育德博士

中華民國一百年十一月

新穎正交分頻多重存取系統之測距方式
A Novel Ranging Method for OFDMA Systems

研究生：林坤昌

Student : Kuhn-Chang Lin

指導教授：蘇育德博士

Advisor : Dr. Yu T. Su

國立交通大學
電信工程學系
碩士論文

A Thesis
Submitted to Department of Communications Engineering
College of Electrical and Computer Engineering
National Chiao Tung University
in partial Fulfillment of the Requirements
for the Degree of
Master of Science
in

Communications Engineering

November 2011

Hsinchu, Taiwan, Republic of China

中華民國一十年十一月

新穎正交分頻多重存取系統之測距方式

學生：林坤昌

指導教授：蘇育德博士

國立交通大學電信工程學系碩士班

摘要

正交分頻多重存取系統可根據使用者的多樣性以及時間軸等自由度並搭配合適資源以及能量的分配來有效率的提高頻譜使用效率。在本論文中提出單一正交分頻多重存取系統信號長度之測距信號結構和信號碼設計，並搭配信號提出所對應的信號偵測以及測距方式。首先，在頻譜上利用線性相角旋轉方式可以產生多組測距信號。而這種設計可以改善效能、測量距離和能量外也可提供較好的對抗多使用者信號干擾以及多路徑通道之能力。電腦模擬可以證實設計的信號比現存的架構有以上等優點。

在介紹完利用線性相角旋轉方式產生多組測距信號這種方式後，將介紹測距信號碼之設計。當在設計測距信號碼時，減少錯誤判斷的機率是重要優先目的之一。根據 Bose, Chaudhuri, and Hocquengham (BCH) 碼所衍生之新測距信號，可以提供較多的信號組數。峰值平均功率比也是重要的設計條件之一，而所設計出的信號除了有較低的峰值平均功率比外也有較低的信號相關性，以供接收機偵測信號以及估計所對應的時間誤差。設計的信號碼提供較好的改善效能以及較準確的距離估計。模擬結果顯示設計的信號比隨機二位元信號碼有以上等優點。

兩層式網路由傳統的蜂巢式網路在加上微型基地台所組成，可以提供較好的網路容量以及覆蓋範圍。在全頻譜重複使用的情況下，兩層式網路互相干擾將導致資料之接收錯誤以及測距信號偵測錯誤的機率大幅上升，而這種情況在測距程序上益發明顯。兩階段之微型基地台以及使用者之間上傳信號同步方式因此而生。在第一階段，微型基地台必須透過廣播頻道進行上傳時間誤差信號的廣播。移動使用者必須接收此信號並根據該信號指令將測距信號和基準信號等傳送時間上進行調整。在第二階段，即可採用正常的測距方式進行。舉例而言，上傳時間誤差信號表示微型基地台到傳統蜂巢式之間的傳送延遲。利用兩階段之微型基地台以及使用者之間上傳信號同步方式，大幅改善測距信號的效能。

A Novel Ranging Method for OFDMA Systems

Student : Kuhn-Chang Lin Advisor : Yu T. Su

Department of Communications Engineering
National Chiao Tung University

Abstract

The OFDM-based multiple access (OFDMA) scheme has been shown to be capable of achieving very high spectral efficiency. A key advantage of an OFDMA system is that it can exploit the diversities offered by the time-varying and user(location)-dependent nature of the subchannels via proper scheduling and power/subchannel allocation. In this thesis, we first present a new single-symbol based initial ranging code structure. We also address issues related to the associated signal detection, timing synchronization methods and novel ranging sequences. These sequences are generated by a prototype sequence with proper linear phase rotations in frequency domain. The proposed detection method is capable of detecting single and multiple ranging codes, estimating the corresponding timing offsets and power strengths. Our approach offers improved performance and enhanced robustness against multi-user interference and multipath fading. Computer simulations are provided to assess the effectiveness of the proposed method and its advantages over existing alternatives.

We proceed to present a novel ranging sequence design method in the second of the thesis. When designing ranging sequences, reducing the probability of collision is one of top priorities. Our ranging sequences design is based on the well known Bose, Chaudhuri, and Hocquengham (BCH) codes. The design generate more ranging sequences to increase the ranging opportunities. Peak to Average Power ration (PAPR) is taken into

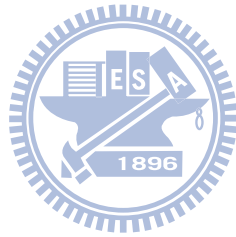
our design consideration as well. Our sequences have the desired properties of rendering low peak to average power ratio (PAPR) and cross-correlation values, which enable a receiver to effectively detect multiple ranging codes and estimate the corresponding time offsets. It therefore gives improved performance and enhanced robustness against multi-user interference and multi-path fading. Numerical results verify the effectiveness of the proposed method and its advantages over that based on pseudo-random binary sequences (PRBS).

The last part of this thesis considers a two-tier pico/femtocell network comprising a conventional cellular network plus embedded pico/femtocell stations. Such network architecture offers an economically viable solution to achieving high cellular capacity and improved coverage. For an OFDMA network using universal frequency reuse and time-division duplex (TDD), however, the resulting cross-tier interference causes unacceptable high outage probability and ranging signal detection error. The problem becomes more critical when performing a ranging process. A two-step uplink synchronization method is provided for uplink synchronization between a mobile station (MS) and a pico/femto base station (BS) that overlays upon a macro/micro cellular network. By using the proposed uplink synchronization method, a unified synchronous ranging channel may be used for ranging and UL access in pico/femtocells with reduced interference.

誌 謝

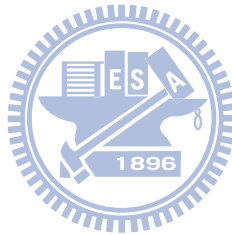
首先感謝指導教授蘇育德博士的指導，並給予我這麼多出國機會跟外界接觸。感謝口試委員吳文榕博士、楊谷章博士以及魏存毅博士給予寶貴的意見讓論文更完善。非常感謝 PK, IK, YS, CY 和 Paul 等博士的指導，使我思考的角度不單只是學術這一方，增加了業界的看法。感謝實驗室的 94 學長姐和 95 的同學，那段時間，應該是學生生涯最快樂的時間。感謝學弟妹可以讓我有指導別人的機會，以及練習溝通的能力。

最後，感謝我的爸媽，可以容忍個性強烈的小孩，沒有他們今天我應該也不會有這個學位。並對我的女朋友等關心我的人，獻上此論文代表我最深的敬意。



Contents

Chinese Abstract	i
English Abstract	ii
Acknowledgements	iv
Contents	v
List of Figures	vii
List of Tables	ix
Abbreviations and Acronyms	x
1 Introduction	1
2 Ranging Signal Design and its Detection for OFDMA Systems	5
2.1 Ranging Process	5
2.2 Channel Assignment Scheme (CAS) and System Model	8
2.3 Ranging Signal Structure	10
2.4 Ranging method	11
2.4.1 Multi-user Ranging Signal Detection and Timing Offset Estimation	13
2.5 Simulation Result and Discussion	15
2.5.1 Simulation Setup	15
2.5.2 Multi-User Detection Performance	16



2.5.3	Performance of Timing Estimator	18
2.5.4	Power Estimator Performance	19
3	Ranging Sequence Design	21
3.1	Introduction to Binary BCH Codes	21
3.2	Ranging Sequences Construction	23
3.3	Multi-user Ranging Signal Detection and Timing Offset Estimation	26
3.4	Simulation Result and Discussion	29
3.4.1	Simulation Setup	29
3.4.2	PAPR Performance	30
3.4.3	Multi-User Detection Performance	31
3.4.4	Performance of Timing Estimator	32
4	Two-step UL Synchronization for Pico/Femtocells	34
4.1	Overlaid Network	34
4.2	UL Network Timing Synchronization	35
4.3	simulation result and discussion	39
4.3.1	Simulation Setup	39
4.3.2	Simulation result	39
5	Conclusion	41
	Bibliography	43

List of Figures

2.1	Ranging and automatic adjustments procedure in IEEE 802.16e-2004 . . .	7
2.2	The round trip delay causes severe timing offset	8
2.3	Interleaved-subband channel assignment scheme for the case, $N_{gp} = 6$ and $N_b=6$	9
2.4	Illustration of MUSIC algorithm in multi-user ranging signal detection and timing offset estimation	15
2.5	Probability of false alarm as a function of average SNR.	17
2.6	Detection probability performance as a function of average SNR.	18
2.7	Timing jitter behavior as a function of average SNR.	19
2.8	Normalized MSE performance of power estimate.	20
3.1	CCDF performance of proposed sequences and PRBS.	30
3.2	Probability of false alarm as a function of average SNR.	31
3.3	Detection probability performance as a function of average SNR.	32
3.4	Timing jitter behavior as a function of the average SNR.	33
4.1	Illustration to a hierarchical cell structure of macro/microcells and pico/femtocells in a cellular OFDM communication system	35
4.2	DL and UL subframes and transmission timing in cellular OFDM com- munication system	36
4.3	Timing misalignment is caused by TTG adjustment.	37

4.4 The false detection probability as a function of distance between fBS and
mBS. 40



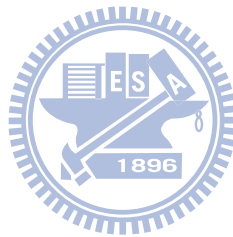
List of Tables

- 2.1 System Parameter 16
- 3.1 BCH parameters 21
- 3.2 BCH codes 23
- 4.1 Parameters of padded Zadoff-Chu sequences 39



Contents

Chinese Abstract	i
English Abstract	ii
Acknowledgements	iv
Contents	v
List of Figures	vii
List of Tables	ix
Abbreviations and Acronyms	x
1 Introduction	1
2 Ranging Signal Design and its Detection for OFDMA Systems	5
2.1 Ranging Process	5
2.2 Channel Assignment Scheme (CAS) and System Model	8
2.3 Ranging Signal Structure	10
2.4 Ranging method	11
2.4.1 Multi-user Ranging Signal Detection and Timing Offset Estimation	13
2.5 Simulation Result and Discussion	15
2.5.1 Simulation Setup	15
2.5.2 Multi-User Detection Performance	16



2.5.3	Performance of Timing Estimator	18
2.5.4	Power Estimator Performance	19
3	Ranging Sequence Design	21
3.1	Introduction to Binary BCH Codes	21
3.2	Ranging Sequences Construction	23
3.3	Multi-user Ranging Signal Detection and Timing Offset Estimation	26
3.4	Simulation Result and Discussion	29
3.4.1	Simulation Setup	29
3.4.2	PAPR Performance	30
3.4.3	Multi-User Detection Performance	31
3.4.4	Performance of Timing Estimator	32
4	Two-step UL Synchronization for Pico/Femtocells	34
4.1	Overlaid Network	34
4.2	UL Network Timing Synchronization	35
4.3	simulation result and discussion	39
4.3.1	Simulation Setup	39
4.3.2	Simulation result	39
5	Conclusion	41
	Bibliography	43



List of Figures

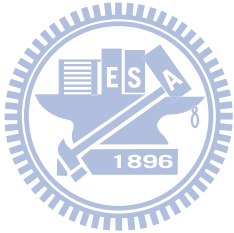
2.1	Ranging and automatic adjustments procedure in IEEE 802.16e-2004 . . .	7
2.2	The round trip delay causes severe timing offset	8
2.3	Interleaved-subband channel assignment scheme for the case, $N_{gp} = 6$ and $N_b=6$	9
2.4	Illustration of MUSIC algorithm in multi-user ranging signal detection and timing offset estimation	15
2.5	Probability of false alarm as a function of average SNR.	17
2.6	Detection probability performance as a function of average SNR.	18
2.7	Timing jitter behavior as a function of average SNR.	19
2.8	Normalized MSE performance of power estimate.	20
3.1	CCDF performance of proposed sequences and PRBS.	30
3.2	Probability of false alarm as a function of average SNR.	31
3.3	Detection probability performance as a function of average SNR.	32
3.4	Timing jitter behavior as a function of the average SNR.	33
4.1	Illustration to a hierarchical cell structure of macro/microcells and pico/femtocells in a cellular OFDM communication system	35
4.2	DL and UL subframes and transmission timing in cellular OFDM com- munication system	36
4.3	Timing misalignment is caused by TTG adjustment.	37

4.4 The false detection probability as a function of distance between fBS and
mBS. 40



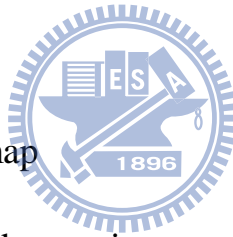
List of Tables

- 2.1 System Parameter 16
- 3.1 BCH parameters 21
- 3.2 BCH codes 23
- 4.1 Parameters of padded Zadoff-Chu sequences 39



Abbreviations and acronyms

BCH code	Bose, Chaudhuri, and Hocquengham code
BPSK	binary phase shift keying
BS	base station
CAS	channel assignment scheme
CFO	carrier frequency offset
CP	cyclic prefix
DL	downlink
DL-MAP	downlink map
DSS	data subscriber station
EC	equivalent class
FFT	fast Fourier transform
HPA	high power amplifier
ICFO	integer carrier frequency offset
ICI	inter subcarrier interference
IFFT	inverse fast Fourier Transform
ISI	inter symbol interference



LTE	long term evolution
MS	mobile station
MSE	mean square error
MUSIC	multiple signal classification
OFDMA	orthogonal frequency division multiple access
PAPR	peak to average power ration
PRBS	pseudo-random binary sequence
RS code	Reed-solomon code
RSS	ranging subscriber station
SS	subscriber station
RTG	receive transition gap
TDD	time division duplex
TTG	transmit transition gap
UL	uplink
UL-MAP	uplink map
ZC code	Zadoff-Chu codes



Chapter 1

Introduction

“Ranging” refers to the task of estimating the distance between a user and the serving base station (BS). Assuming the availability of a direct line-of-sight (LOS) link, we can relate the timing offset and the (slant) range of the link by the fact that the former is equal to the ratio of the distance and the light speed. In this sense, “ranging” is equivalent to discovering the timing offset between the user and the serving base station as well. As in most circumstances, there exists no LOS link, ranging has more to do with the timing synchronization process in a cellular network.

For OFDMA systems, timing offset will not only cause inter symbol interference but also inter subcarrier interference. To avoid so, any user that attempts to create a communication link is required to carry out a successful initial ranging process with the base station. The whole ranging process can be decomposed into several steps. First of all, once a user senses a BS, for network entry it first scans for a Down Link (DL) channel and synchronizes itself with the preambles of the serving BS. After synchronization, the user shall have the knowledge of critical parameters from DL-MAP and UL-MAP, and then performs initial ranging process. Even if the DL synchronization is perfect, the round trip delay can not be compensated by user without help of BS. The goal of the initial ranging is to compensate the timing offset. In initial ranging, the Ranging Subscriber Station (RSS) chooses one of the available ranging codes randomly and transmits it back to the BS. The RSS should transmit the ranging code at a random time during

the Up Link (UL) frame as long as there is a ranging opportunity. UL-MAP will show if a ranging opportunity is available through the next UL frame. However, the RSS will not notice which ranging code is chosen such that the collision is inevitable. However, this issue can be conquered by increasing the ranging opportunities. At the receiver side, the BS is required to detect different received ranging codes, estimate the timing offset for each RSS that bears an initial ranging code. The BS then broadcasts the detected ranging codes with adjustments for the timing correction. The status notifications of either ranging successful or retransmission are also broadcasted.

Several studies on the initial ranging for an OFDMA system like that specified by the IEEE 802.16e standard [2] have been reported [3]-[7]. These works fall into two major categories. The first category [3] is based on the ranging codes given in [2]. The second category [5]-[7] proposes new ranging code structures. Zhuang *et al.* [5] divided all active ranging subscriber stations (RSSs) into different groups. Each group is given its specific and non-overlapping subchannels, which consists of consecutive adjacent subcarriers. As consecutive subcarriers are assigned to an user, diversity is lacking. Frequency-selective fading and propagation delay variation of RSSs further degrade the performance. [6] suggested an interleaved channel assignment scheme to overcome the major drawbacks of the above approaches. However, multiple OFDMA symbols are needed and the carrier frequency offsets (CFOs) between the received signals and the BS local reference is not taken into account and perfect frequency alignment among all RSSs and the BS is assumed instead. Such an assumption is not realistic and ignores the fact that the residual CFOs cause the loss of orthogonality among ranging codes and are likely to induce severe performance degradation. Sanguinetti *et al.*[7] employed a MUSIC-like [8] algorithm to fix the problem at the cost of a longer ranging ranging signal duration (and therefore lower system throughput). Guard bands between neighboring subbands of different ranging channels are also needed to prevent interference from other groups. We propose a specific ranging channel assignment a new class of frequency domain ranging

codes which enables the BS to employ a MUSIC-like algorithm to detect multiple RSSs and estimate their timing offsets. Our design uses only one OFDM symbol; guard bands between ranging channels are not needed and the associated receive algorithm gives robust, excellent multi-user detection and timing estimation performance. Compared with the existing solutions, our proposal is more spectral efficient, yields improved performance and offers greater immunity against the multiuser interference and frequency selective fading.

In ranging sequence design, we present a novel systematic method to generate ranging sequences based on BCH codes. The method is capable of generating large number of ranging sequences to increase the ranging opportunities and reduce the collision probability. Ranging process consists of initial, periodic, and handover ranging procedures. Initial ranging procedure is more troublesome than others but dedicated for non-synchronized users. However, our proposed approach can be applied to other ranging processes without any modification. Our method also results in lower cross-correlation and PAPRs when compared with existing ranging sequence sets. As our approach is based on systematic BCH codes, the required storage space is much smaller than those required by other methods as we need only to store the information part of a sequence. Lower crosscorrelation gives a better detection probability and smaller false alarm probability especially if there are multiple incoming ranging sequences. On the other hand, lower PAPR values enhances the power efficiency of mobile subscribers and reduces the in-band interference caused by the transmitters clipping operation.

A femtocell serves as a small range and is installed as a data access point around high user density hotspots for low-mobility users. A femtocell is distributed randomly over the coverage of the macorcell. The femtocell radio range (10 - 50 meters) is much smaller than the macrocell radius (300 - 2000 meters). Users transmitting to femtocells experience superior signal reception and lower their transmit power, consequently prolonging battery life. Although transmission power from femto users and femto station is

reduced, it still causes severe cross-tier interference to macro users which are close to the femto station. With universal frequency reuse and time-division duplex (TDD) OFDMA transmission however, the synchronization will become an important and critical issue. For example, for a macro user, the signal from macro station will be contaminated the signal from the femto station and femto station if the network synchronization is not well-done. The interference level depends on the distance between the macro user and the femto station. The cross-tier interference causes unacceptable outage probability and ranging signal detection error. A two-step uplink synchronization method is provided for uplink synchronization between a mobile station a pico/femto base station that is deployed together with an overlay macro/micro station. In a first step, the pico/femto BS encodes and broadcasts UL transmission time advance offset information via broadcast channel. The MS decodes the received UL transmission timing advance offset information and advances its uplink timing for uplink ranging or reference signal, transmission based on the decoded offset value. In a second step, the MS and the pico/femto performs regular uplink synchronization and uplink access. In one example, the UL transmission timing advance offset information indicates a round-trip propagation of radio signals between the pico/femto vase station and the overlay maco/micro base station. By using the two-step uplink synchronization method, a unified synchronous ranging channel bay be used for ranging and UL access in pico/femrocells with reduce interference.

Notation: $\lfloor \cdot \rfloor$ and j denote the floor operation and $\sqrt{-1}$. $(\cdot)^{\mathbf{T}}$ and $(\cdot)^{\mathbf{H}}$ denote transpose and Hermitian operations.

Chapter 2

Ranging Signal Design and its Detection for OFDMA Systems

2.1 Ranging Process

Before an Long Term Evolution (LTE) terminal can communicate with an LTE network it has to do the followings [4]:

1. Find and acquire synchronization to a target cell within the network.
2. Receive and decode the information, also referred to as the cell system information, needed to communicate with and operate properly within the cell.

Once the system information has been correctly decoded, the terminal can access the cell by means of the so-called random-access procedure. The so-called random-access procedure of LTE is one ranging process and can be concluded as follows:

1. The ranging user transmits a random-access preamble (ranging preamble) to the target BS such that the target BS can estimation the transmission timing of the ranging user.
2. The BS will broadcast the timing advance command and the ranging user shall follow this command and adjust its timing. In addition to establishing uplink synchronization, the second step also assigns uplink resources to the terminal to be used in the third step in the random-access procedure.

3. The ranging user sends its identity to the network using pre-allocated channel. The exact content of this signaling depends on the state of the terminal, in particular whether it is previously known to the network or not.
4. The BS will broadcast a contention-resolution message from the network to the terminal. This step also resolves any contention due to multiple terminals trying to access the system using the same random-access resource.

For the interested readers, more detailed information can be found in [4]. Similarly, as shown in figure 2.1, it is a ranging and automatic adjustments procedure in IEEE 802.16e-2004. Due to many sophisticated technical terms, we conclude the ranging process as follows. Any user that attempts to create a communication link is required to carry out a successful initial ranging process with the base station (BS). Once a user senses a BS, for network entry it first scans for a Down Link (DL) channel and synchronizes itself with the preambles of the serving BS. After synchronization, the user shall have the knowledge of critical parameters from DL-MAP and UL-MAP, and then performs initial ranging process. Even if the DL synchronization is perfect, the round trip delay can not be compensated by RSS.

The goal of the initial ranging is to compensate the timing offset. In initial ranging, the RSS chooses one of the available ranging codes randomly and transmits it back to the BS. The SS should transmit the ranging code at a random time during the Up Link (UL) frame as long as there is a ranging opportunity. UL-MAP will show if a ranging opportunity is available through the next UL frame. However, the RSS will not notice which ranging code is chosen such that the collision is inevitable. However, this issue can be conquered by increasing the ranging opportunities. At the receiver side, the BS is required to detect different received ranging codes, estimate the timing offset for each RSS that bears an initial ranging code. The BS then broadcasts the detected ranging codes with adjustments for the timing correction. The status notifications of either ranging successful or retransmission are also broadcasted.

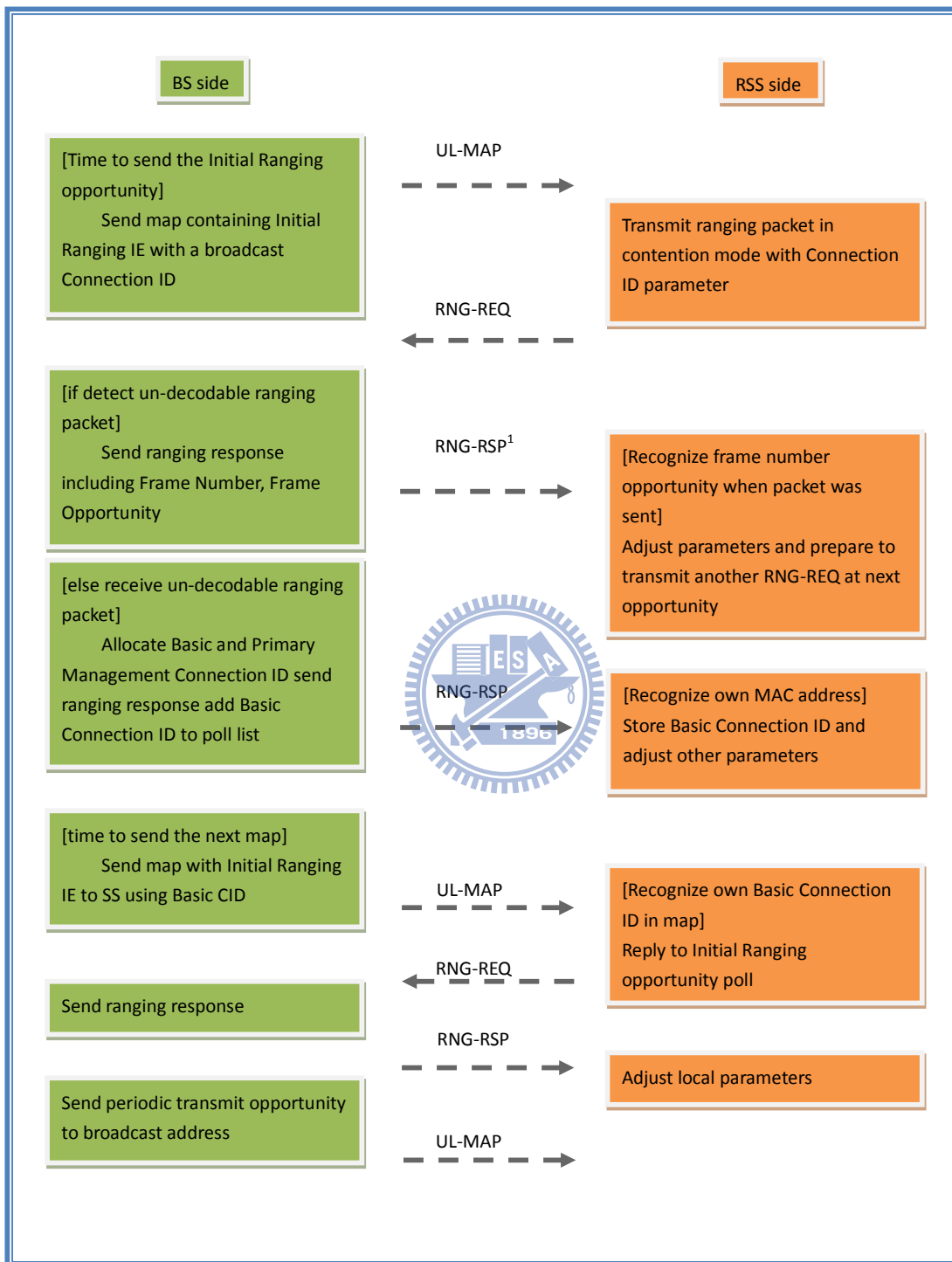


Figure 2.1: Ranging and automatic adjustments procedure in IEEE 802.16e-2004

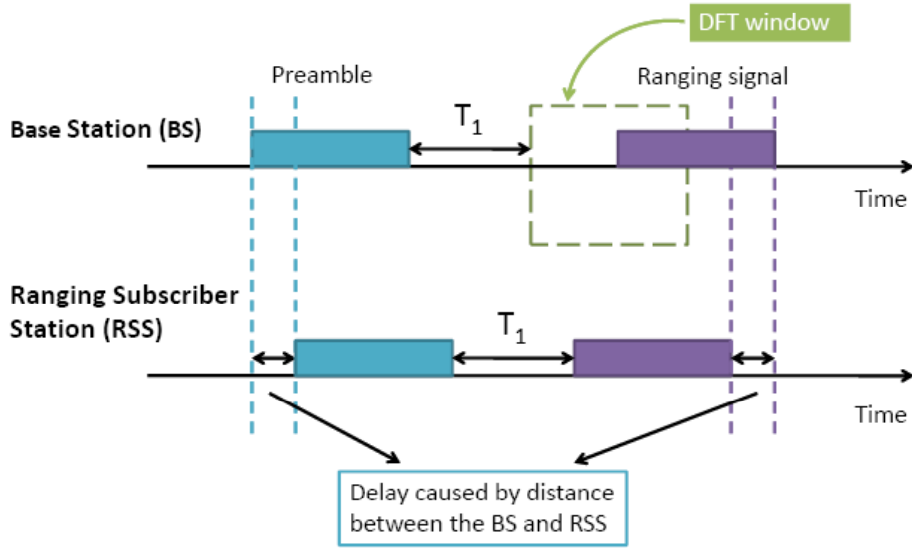


Figure 2.2: The round trip delay causes severe timing offset

2.2 Channel Assignment Scheme (CAS) and System Model

Subcarriers assigned for RSSs are divided into N_{gp} groups with each group having N_b subbands and each subband consisting of N_c consecutive subcarriers such that each group can support a maximum of M RSSs. Our design has two major advantages. The RSS can choose one suitable group to transmit based on channel condition from DL received signal strength. The other is detection complexity reduction. There is no overlapping subcarriers among each group such that the simpler energy detector can be applied as a trigger. If the energy detector outputs are less than a specific threshold, we could skip checking these group.

Let S_p be the set of indices of the subcarriers allocated to the p th group and denote by R_{ip} the i th RSS in the p th group which employs the frequency domain ranging code

$\{C_{ip}(u) : u = 1, \dots, N_b N_c\}$. Let f_s be the lowest subcarrier index allocated for RSSs.

For $0 \leq p \leq N_{gp} - 1$, S_p is

$$S_p = \{f_s + pN_c + \iota D_b + \nu : 0 \leq \iota \leq N_b - 1, 0 \leq \nu \leq N_c - 1\}, \quad (2.1)$$

where D_b denotes the frequency spacing between subbands. The frequency domain ranging signal $X_{ip}(k)$ for R_{ip} is defined as

$$X_{ip}(k) = \begin{cases} A_{ip} C_{ip}(u), & k \in S_p, u = 1, 2, \dots, N_b N_c \\ 0, & \text{otherwise,} \end{cases} \quad (2.2)$$

where $|C_{ip}(u)| = 1$ and A_{ip} is the relative amplitude of R_{ip} .

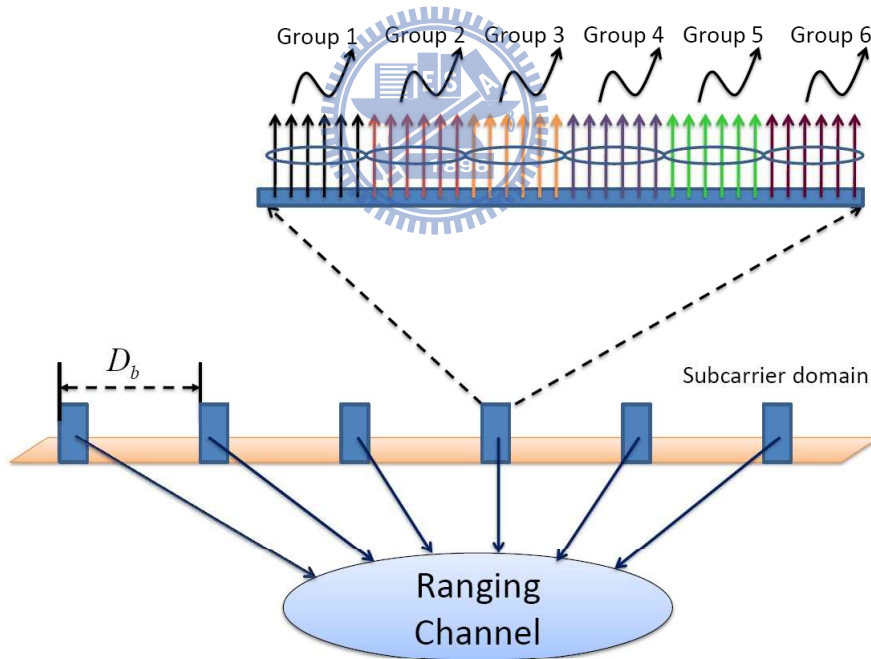


Figure 2.3: Interleaved-subband channel assignment scheme for the case, $N_{gp} = 6$ and $N_b=6$.

The maximum transmission delay D_{max} (samples) equals to the round-trip propagation delay between the BS and a RSS at the boundary of the cell. To avoid inter-subcarrier interference (ICI) and inter symbol interference (ISI), the length of the cyclic prefix (CP), N_g , must be larger than the sum of D_{max} and the maximum delay spread among all uplink ranging channels L (samples) [9]. This assumption is not restrictive, since in many standardized OFDM systems the initialization blocks are usually preceded by extended CPs. With the extended CP inserted, the time domain ranging signal for R_{ip} is $x_{ip}(n)$, $n = -N_g, -N_g + 1, \dots, N$, where N is the FFT size.

Assuming the uplink channels remain static within a symbol duration and ignoring the presence of noise for the moment, we express the received ranging waveform $y_{ip}^R(n)$ for R_{ip} as

$$y_{ip}^R(n) = \sum_{l=0}^{L-1} h_{ip}(l)x_{ip}(n-l) \quad (2.3)$$

where $h_{ip}(l)$, $l = 0, \dots, L-1$ are the associated channel tap weights. The remaining $N - N_{gp}N_cN_b$ subcarriers are assigned to N_{DSS} data subscriber stations (DSSs) which have already completed their initial ranging process and are assumed to be perfectly synchronized with the BS' time and frequency scales. $y_i^D(n)$ denotes the signal of the i th DSS. The received signal at the BS thus becomes

$$y(n) = \sum_{p=0}^{N_{gp}-1} \sum_{i=0}^{M-1} y_{ip}^R(n - d_{ip})e^{j2\pi\varepsilon_{ip}n/N} + \sum_{i=0}^{N_{DSS}-1} y_i^D(n) + w(n) \quad (2.4)$$

where $\{w(n)\}$ are independent and identical distributed (i.i.d.) complex circular symmetric Gaussian random variables with mean zero and variance $\sigma_w^2 = E[|w(n)|^2]$ and d_{ip} , ε_{ip} represent the timing offset and normalized frequency offset of R_{ip} .

2.3 Ranging Signal Structure

The maximum number of RSSs supported by one group, M , can be expressed as

$$M = \min\{[N/N_g], \min\{N_b, N_c\} - 1\} \quad (2.5)$$

In practice, $\lceil N/N_g \rceil$ is usually larger than 2, hence a judicious choice of $\{N_b, N_c\}$ is needed to ensure $M > 2$.

The ranging code in the i th subband, C_{ip}^i , for the R_{ip} is given by

$$C_{ip}^i(\nu) = e^{-j2\pi i\nu/M}, \nu = 0, 1, \dots, N_c - 1. \quad (2.6)$$

The same ranging code can be transmitted using different subcarrier group without causing any interference for the subcarriers allocated are disjoint. Our design does not ensure orthogonality among codes in the same group. When choosing the i th ranging code, the phase difference between two consecutive assigned subcarriers are rotated by $-2\pi i/M$. The phase rotation caused by round-trip delay and channel delay spread is between 0 and $-2\pi/M$. This implies that the overall frequency-domain phase shifts of all RSSs in the same group are non-overlapping over $\left[\frac{-2i\pi}{M}, \frac{-2(i+1)\pi}{M}\right]$, where $i = 0, 1, \dots, M - 1$. By using the MUSIC algorithm [8], we perform one-to-one mapping from the overall phase shifts of RSSs in the same group into the corresponding RSSs associated with the detected peak positions. We can simultaneously obtain the delay information of R_{ip} from the overall phase shift without additional complicated computations. The RSSs in the same group can thus be easily detected and decoupled without using multiple OFDMA symbols.

2.4 Ranging method

Our estimate assume that the timing offset d_{ip} for R_{ip} is equal to the sum of the round-trip transmission delay and the channel group delay. When a RSS receives the timing offset estimate from the BS, it adjusts its timing accordingly and retransmit its ranging code with both cyclic prefix and postfix to avoid inter carrier interference (ICI).

The code structure of (2.6) and the assumption that the subband bandwidth is smaller than the uplink channel's coherent bandwidth implies that the equivalent channel

gains within a the ι th subband of R_{ip} are related by

$$H_{ip}^\iota(\nu) \approx H_{ip}^\iota(0)e^{-j2\pi\nu(\frac{i}{M} + \frac{d_{ip}}{N})}, \nu = 1, \dots, N_c - 1 \quad (2.7)$$

Let \mathbf{Y}_p^ι be the N_c -dimensional vector that collects the components of the DFT output vector corresponding to the ι th subband of the p th group. Since the DSSs are assumed to be perfectly synchronized to the BS time reference, their signals will not contribute to \mathbf{Y}_p^ι , we have

$$\mathbf{Y}_p^\iota = \sum_{i=0}^{M-1} \mathbf{F}(\varepsilon_{ip}) \mathbf{v}_{ip} H_{ip}^\iota(0) + \mathbf{n}_p^\iota \quad (2.8)$$

where \mathbf{n}_p^ι is the sum of white Gaussian noise and the interference from the nearby groups and \mathbf{v}_{ip} is given by

$$\mathbf{v}_{ip} = \left(1, e^{-j2\pi(\frac{i}{M} + \frac{d_{ip}}{N})}, \dots, e^{-j2\pi(N_c-1)(\frac{i}{M} + \frac{d_{ip}}{N})} \right)^\mathbf{T}. \quad (2.9)$$

Furthermore, $\mathbf{F}(\varepsilon_{ip})$ is a $N_c \times N_c$ Toeplitz matrix with the element in a th row and the b th column given by [9]

$$f_{a,b}(\varepsilon_{ip}) = \frac{\sin(\pi(a-b+\varepsilon_{ip}))}{N \sin(\pi(b-a+\varepsilon_{ip})/N)} e^{j\pi(b-a+\varepsilon_{ip})(N-1)/N} \quad (2.10)$$

A RSS intending to start initial ranging should first derive its initial frequency and timing estimates from a downlink control signal broadcasted by the BS. This means the CFOs are only due to Doppler shifts and/or estimation errors whence are assumed to lie within a small fraction of the subcarrier spacing, i.e., $|\varepsilon_{ip}| \approx 0$, and $\mathbf{F}(\varepsilon_{ip})$ in (2.8) can be replaced with \mathbf{I}_{N_c} , where \mathbf{I}_{N_c} is an identity matrix of order N_c . When $|\varepsilon_{ip}| \ll 1$, $\mathbf{F}(\varepsilon_{ip})$ can be viewed as a tri-diagonal matrix. In this case, $\mathbf{F}(\varepsilon_{ip}) \mathbf{v}_{ip} H_{ip}^\iota(0) \approx \mathbf{v}_{ip} \tilde{H}_{ip}^\iota(0)$ with the exceptions of the highest and lowest indexed terms. By combing these small deviation terms with \mathbf{n}_p^ι to form $\tilde{\mathbf{n}}_p^\iota$, we rewrite (2.8) as

$$\mathbf{Y}_p^\iota = \sum_{i=0}^{M-1} \mathbf{v}_{ip} \tilde{H}_{ip}^\iota + \tilde{\mathbf{n}}_p^\iota, \iota = 0, 1, \dots, N_b - 1 \quad (2.11)$$

which can be expressed in a more compact form

$$\mathbf{Y}_p = (\mathbf{Y}_p^0 \ \mathbf{Y}_p^1 \ \cdots \ \mathbf{Y}_p^{N_b-1}) = \mathbf{V}_p \tilde{\mathbf{H}}_p + \tilde{\mathbf{N}}_p \quad (2.12)$$

where \mathbf{Y}_p is the matrix obtained by stacking up the received samples from subbands within the p th group, $\mathbf{V}_p = (\mathbf{v}_{0p} \ \mathbf{v}_{1p} \ \cdots \ \mathbf{v}_{(M-1)p})$, $\tilde{\mathbf{N}}_p = (\tilde{\mathbf{n}}_p^0 \ \tilde{\mathbf{n}}_p^1 \ \cdots \ \tilde{\mathbf{n}}_p^{N_b-1})$, and

$$\tilde{\mathbf{H}}_p = \begin{pmatrix} \tilde{H}_{0p}^0 & \tilde{H}_{0p}^1 & \cdots & \tilde{H}_{0p}^{N_b-1} \\ \vdots & \vdots & \ddots & \vdots \\ \tilde{H}_{(M-1)p}^0 & \tilde{H}_{(M-1)p}^1 & \cdots & \tilde{H}_{(M-1)p}^{N_b-1} \end{pmatrix}. \quad (2.13)$$

2.4.1 Multi-user Ranging Signal Detection and Timing Offset Estimation

The fractional frequency offset results in inter-carrier interference (ICI) to subbands in the nearby group. Let E_p be the energy (i.e., the magnitude square of the DFT output) of the p th subcarrier group excluding the highest and lowest indexed subcarriers of each subband. In the absence of signal, E_p is a chi-square distributed with $2N_b(N_c-2)$ degrees of freedom. When the noise variance is known, the desired false alarm probability can be achieved by selecting a proper η_0 . We check $E_p > \eta_0$ first to see if subsequent operations are needed.

The covariance matrix of \mathbf{Y}_p is defined by $\Phi_p = \frac{1}{N_b} \mathbf{Y}_p \mathbf{Y}_p^H$. When there are κ_p RSSs in the p th group, $\kappa_p \leq M$, we have $N_c - \kappa_p$ basis vectors which span the null space \mathbf{U}_{wp} and can be obtained by performing singular value decomposition (SVD) on Φ_p . Assuming $\hat{\kappa}_p = M$ we compute

$$\Upsilon(d) = \frac{\|\alpha^H(d)\alpha(d)\|}{\|\alpha^H(d)\mathbf{U}_{wp}\mathbf{U}_{wp}^H\alpha(d)\|}, \quad d = 0, \dots, N-1. \quad (2.14)$$

where $\alpha(d) = (1, e^{-j2\pi d/N}, \dots, e^{-j2\pi d(N_c-1)/N})^T$, and find the local maximums. These peak values correspond to the ratio of the total energy to the energy projecting onto

the null space. There is an one-to-one correspondence between the local peaks and the active RSS's delays. Therefore, we make a decision about R_{ip} according to whether there is a peak located within $\{Ni/M, N(i+1)/M\}$.

The vector $\hat{\mathbf{d}}_{\mathbf{p}} = (\hat{d}_{0p}, \hat{d}_{1p}, \dots, \hat{d}_{(M-1)p})^T$, which includes information about the number of the active RSSs in the p th group and their delays, is obtained by the following algorithm.

1. Compute E_p based on the received frequency domain samples. If $E_p < \eta_0$, "no signal" is declared and the algorithm terminates.
2. Arrange the frequency domain samples in matrix form $\mathbf{Y}_{\mathbf{p}}$ and set $\hat{\kappa}_p = M$.
3. Apply SVD to $\Phi_{\mathbf{p}}$, find the $N_c \times (N_c - \hat{\kappa}_p)$ matrix $\hat{\mathbf{U}}_{\mathbf{wp}}$ and then $\Upsilon(d)$.
4. Find the largest $\hat{\kappa}_p$ peaks of $\Upsilon(d)$ and compare these local peak values with the threshold, $\eta_1(N_c, N_b, \hat{\kappa}_p)$. If there exist l peaks below the threshold, $\hat{\kappa}_p \leftarrow \hat{\kappa}_p - l$ and go back to Step 3). The threshold is determined numerically.
5. Based on the local peak positions, we determine if an RSS R_{ip} is active and its timing offset \hat{d}_{ip} is obtained by subtracting Ni/M from the peak position.

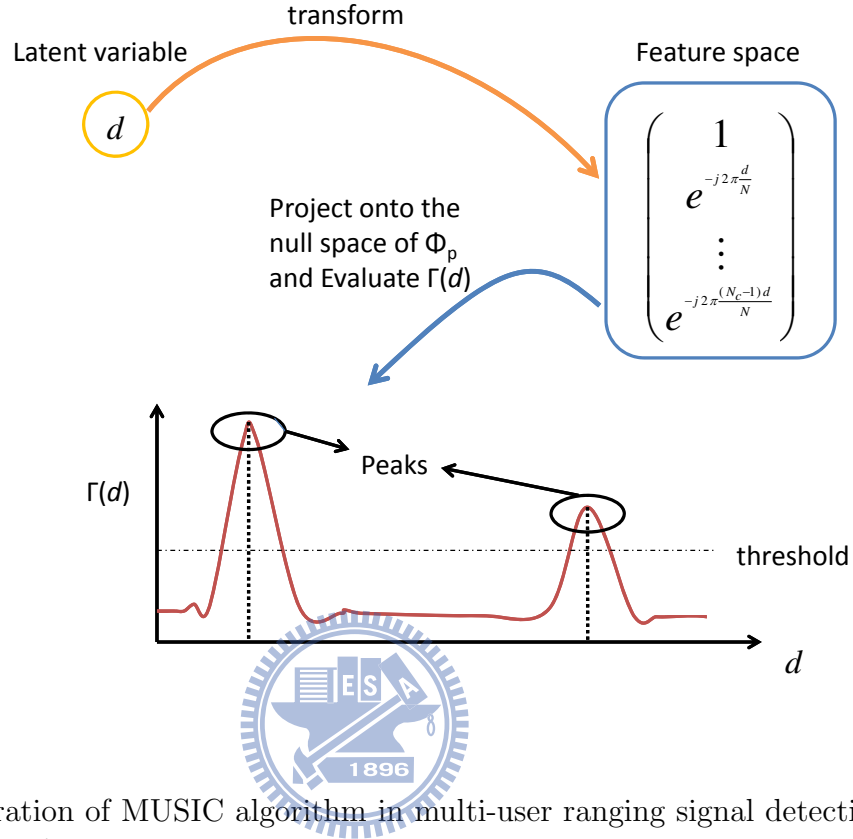


Figure 2.4: Illustration of MUSIC algorithm in multi-user ranging signal detection and timing offset estimation

2.5 Simulation Result and Discussion

2.5.1 Simulation Setup

The OFDMA system parameters used in the simulations reported in this section are selected from [2] and [12]. The uplink bandwidth is 10 MHz, and the subcarrier spacing is 10.9375 KHz. The FFT size, N , is 1024. ITU Vehicular A channel model is used and the sampling interval, T_s , is 89.285 ns. We consider a cell size of radius 5 km so that the round-trip delay $d_{max}=33.34 \mu s = 373$ samples. N_g is assumed to be 512 samples to satisfy the condition $N_g > d_{max} + L$ and each group supports $M = 2$ RSSs. The subcarriers numbers and OFDM symbols used by one group for our proposal ($N_c =$

6, $N_b = 6$, $N_{gp} = 4$ and $D_b = 140$) and two earlier schemes are summarized in Table 1 where FLM refers to the scheme proposed by Fu, Li and Minn [6] while SMP is an abbreviation for the method proposed by Sanguinetti, Morelli, and Poor [7].

Table 2.1: System Parameter

	Proposed	FLM	SMP
Supported RSS number per group, M	2	2	2
Subcarriers per OFDM symbol ($N_c \times N_b$)	36	36	32
Ranging signal duration (in OFDM symbols)	1	2	3

The supported maximum speed of RSS is 120 Km/hr and carrier frequency is 2.5 GHz. The normalized residual CFOs of RSSs thus lie within the range $[-0.05, 0.05]$ and are assumed to be i.i.d. for different RSSs. Because our proposed algorithm utilizes the FFT output data, the interference mainly come from RSSs in same group and RSSs in the nearby groups. We assume there are K active RSSs in the group and I RSSs in the nearby groups. Some or all of the following RSS distributions are considered: (i) $K = 1$, $I = 0$, (ii) $K = 1$, $I = 1$, (iii) $K = 1$, $I = 2$, (iv) $K = 2$, $I = 0$, and (v) $K = 2$, $I = 2$, within one ranging time-slot.

2.5.2 Multi-User Detection Performance

SNR is defined as the ratio of signal variance to noise variance in time domain. Comparisons are made with FLM and SMP ranging schemes. The results of Fig. 2.5.2 indicates that the proposed scheme performs remarkably better than FLM and SMP because of its intrinsic robustness against CFOs. In FLM scheme, the i th ranging code is declared active provided that the quantity exceeds a suitable threshold η which is proportional to the estimated noise power σ^2 . The fractional RSSs' CFOs destroy the orthogonality in the same group. When a RSS power becomes larger, so are the

interference and the false alarm probability. Hence, the performance is dominated by the interference from the same group.

In the SMP scheme, the interference from the same group is mitigated by employing MUSIC algorithm with extending one more OFDM symbol. However, the interference from nearby groups degrades the performance when the subbands assigned for different groups are adjacent. For alleviating this effect, the guard bands are required. On the other hand, our scheme can find that the RSSs in the different group do not cause increase of false alarm probability even if the residual frequency offset exists. When SNR is lower, both signal and null spaces are influenced by relative large noise. When the SNR > 5 dB, the noise effect becomes insignificant. However, even for SNR < -6 dB, the false alarm probability is still less than 0.02. Fig. 2.5.2 shows the probability of

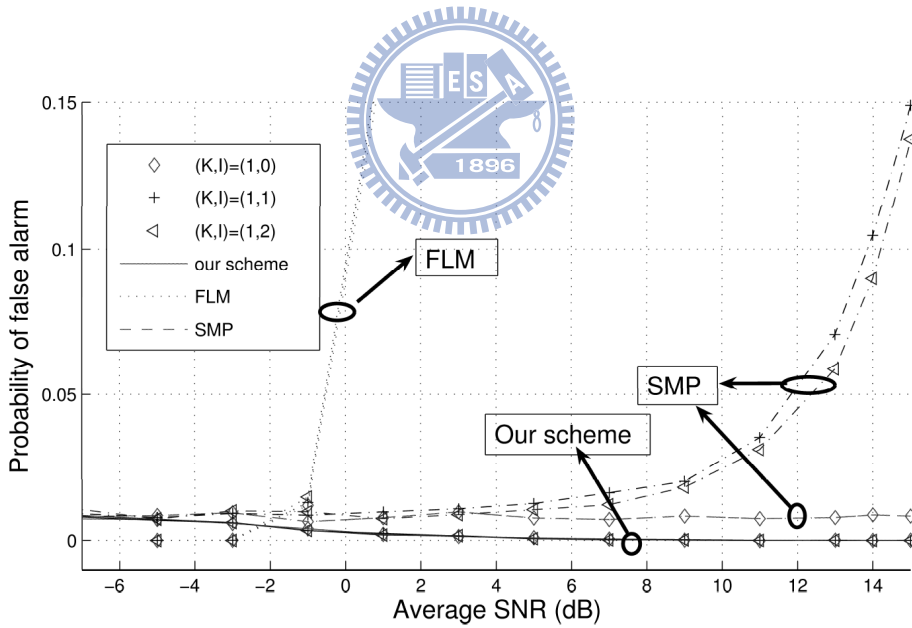


Figure 2.5: Probability of false alarm as a function of average SNR.

correct detection (P_D) performance versus average SNR. As our ranging signal needs only one OFDM symbol the required transmission energy is less than the existing approaches that employ two or more symbols. Our proposal gives near perfect P_D (≈ 1) even if

SNR is as small as -10 dB. The performance degrades slightly if there are two RSSs in the same group. The reason is that the increased active RSS number reduces the dimensionality of the noise subspace. When SNR is larger than -7 dB, the detection performance loss of is less than 0.005.

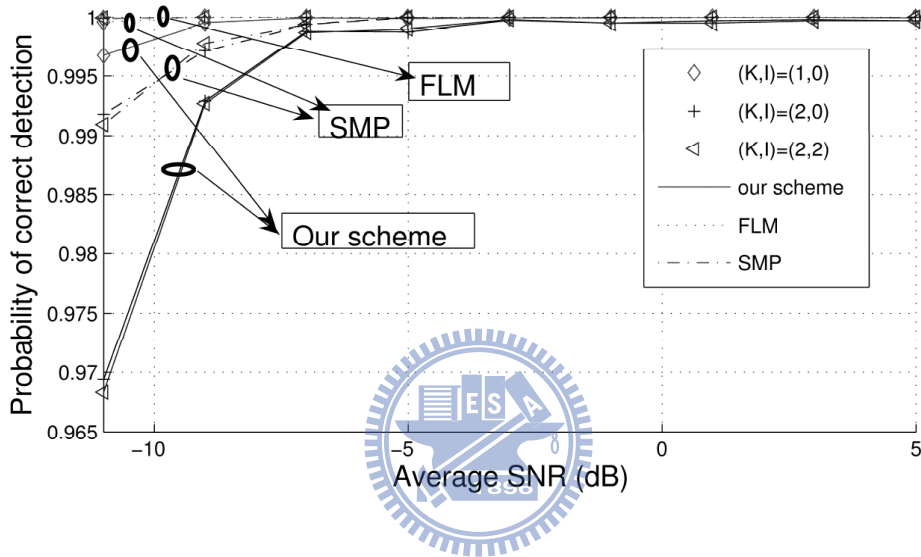


Figure 2.6: Detection probability performance as a function of average SNR.

2.5.3 Performance of Timing Estimator

Fig. 2.5.3 plots the the timing estimation jitter, i.e., the root mean squared timing offset estimation error, as a function of the average SNR for the various RSS distributions. In each simulation run, the true transmission delays are taken randomly from the interval $[0, d_{max}]$. In simulating the FLM scheme, we employ the SEGA algorithm with two iterations. It is observed that one RSS in one group yields better performance than two RSSs in one group. But the performance difference is just one sampling interval. We can see that for SNR larger than 1 dB the proposed and the FLM schemes give almost identical performance. After each RSS has successfully finished initial ranging, adjusted

its timing offset, the BS will be able to support more RSSs in one group for subsequent periodic ranging since most of the round-trip delay uncertainty has been removed and the CP length can be reduced accordingly; see (2.5).

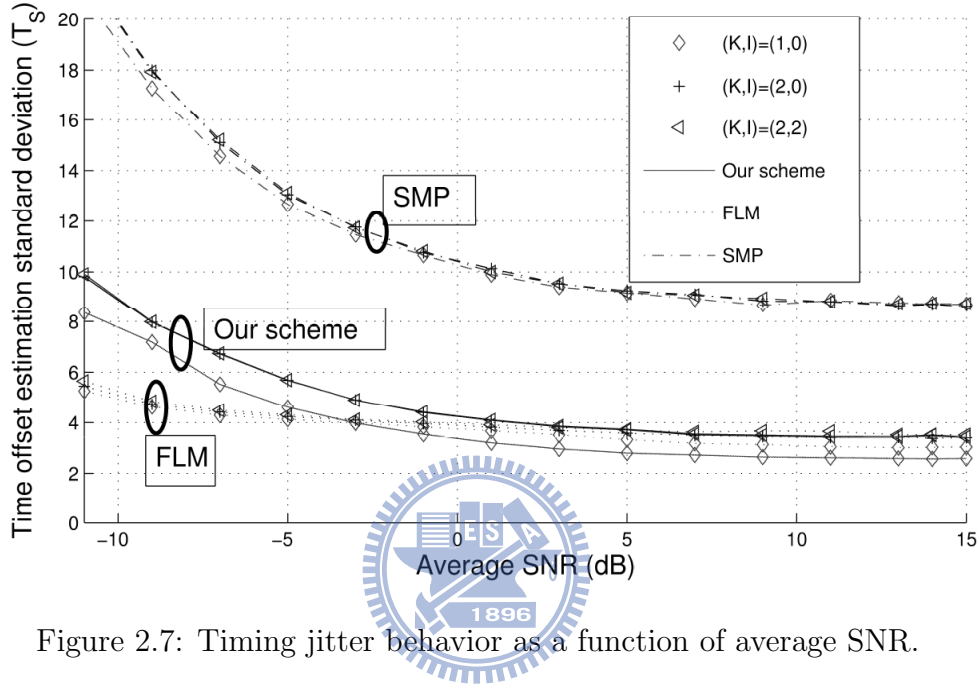


Figure 2.7: Timing jitter behavior as a function of average SNR.

2.5.4 Power Estimator Performance

Fig. 2.5.4 shows the normalized MSE performance of our power estimation scheme as a function of average SNR for various RSS distribution. In lower SNR, our proposed scheme owns nice performance. The MSE curves flatten out at high SNR's due to the limitation of the approximation (2.7).

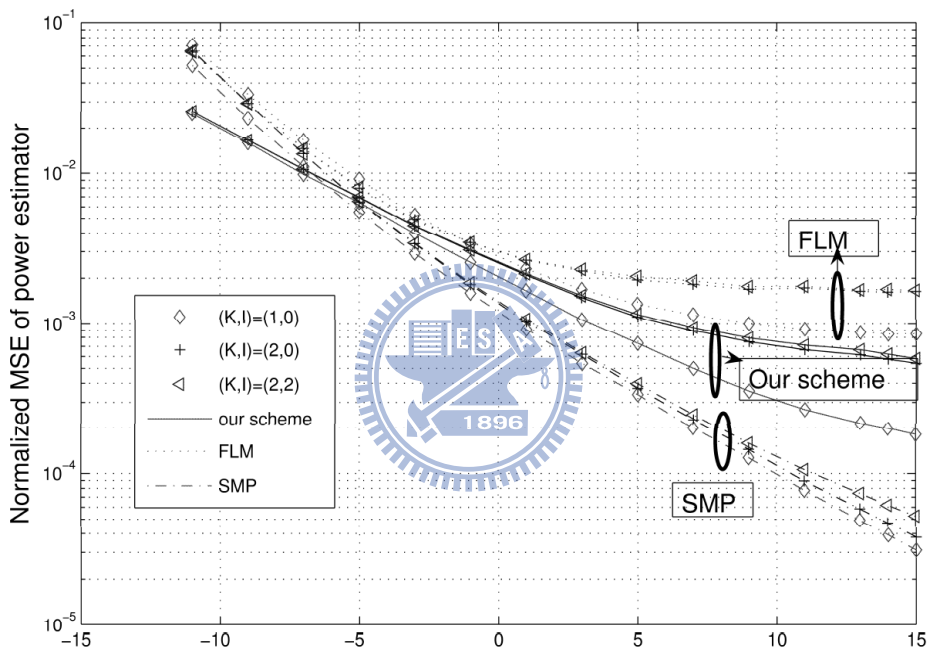


Figure 2.8: Normalized MSE performance of power estimate.

Chapter 3

Ranging Sequence Design

3.1 Introduction to Binary BCH Codes

The Bose, Chaudhuri and Hocquenghem (BCH) codes form a large class of powerful random error-correcting cyclic codes. Reed-solomon (RS) code is one important and well-known subclass of BCH codes. Since we are interested in BPSK-modulated ranging sequences, we shall consider binary primitive BCH codes only. As will become clear later, BCH codes do offer great flexibility for our sequence design. We first recall the basic property of BCH codes: for any positive integers $m(m > 3)$ and $t(t < 2^{m-1})$, there exists a binary BCH code with following parameters:

Table 3.1: BCH parameters

Block length	$n = 2^m - 1$
Number of parity-check digits	$n - k \leq mt$
Minimum distance	$d_{min} \geq 2t + 1$

For t -error-correcting BCH code, it can correct any combination of t or fewer error in n digits. The error-correcting capability depends on the generator polynomial of the chosen BCH and the generator polynomial is specified in terms of its roots from the Galois field $GF(2^m)$. Let α be the a primitive element in $GF(2^m)$. The generator polynomial $g(X)$ of t -error-correcting code has $\alpha, \alpha^2, \alpha^3, \dots, \alpha^{2t}$ and their conjugates as

its root [?]. Therefore, the generator polynomial will be the least common multiple (**LCM**) of the minimum polynomials of α^i 's, $1 \leq i \leq 2t$.

$$g(X) = \mathbf{LCM}\{\phi_1(\mathbf{X}), \phi_2(\mathbf{X}), \dots, \phi_{2t}(\mathbf{X})\} \quad (3.1)$$

Let $f(X)$ be a polynomial with coefficients in $GF(2)$. If β , an element in $GF(2^m)$, is a root of $f(X)$, and then for any $l \geq 0$, β^{2^l} is also the root of $f(X)$. Therefore, if i is even, there exists one i' which $i = i'2^l$. It implies α^i and $\alpha^{i'}$ have the same minimum polynomial. The equation (3.2) can be rewritten as

$$g(X) = \mathbf{LCM}\{\phi_1(\mathbf{X}), \phi_3(\mathbf{X}), \dots, \phi_{2t-1}(\mathbf{X})\} \quad (3.2)$$

Lemma 3.1.1. The Greatest Common Factor (GCF) of $g(X)$ and $X + 1$ is 1.

$$\mathbf{GCF}\{g(X), X + 1\} = 1.$$

Proof. $X+1$ has 1 as its only one root, and it is a minimal polynomial. $g(X)$ is the LCM of $\phi_1(X), \phi_3(X), \dots, \phi_{2t-1}(X)$ excluding $X + 1$. Therefore $\mathbf{GCF}\{g(X), X + 1\} = 1$. \square

With the knowledge of generator polynomial, the desired BCH can be constructed and the parameters of all binary BCH codes of length $2^m - 1$ with $m < 8$ are given the Table 3.2.

BCH codes are cyclic codes and attractive for simpler encoder implementation. The codeword $C(X)$ can be obtained by multiplying message $u(X)$ with $g(X)$ directly. The systematic encoding approach of (n, k, t) BCH code with the generator polynomial $g(X)$ can be carry out as follows:

$$\text{Let } g(X) = 1 + g_1X + g_2X^2 + \dots + g_{n-k-1}X^{n-k-1} + X^{n-k}.$$

1. Premultiply the message $u(X)$ by X^{n-k} .
2. Obtain the remainder $b(X)$ from dividing $X^{n-k}u(X)$ by $g(X)$.
3. Codeword $C(X) = X^{n-k}u(X) + b(X)$.

Table 3.2: BCH codes

n	k	t	n	k	t	n	k	t
7	4	1	63	39	4	127	92	5
15	11	1		36	5		85	6
	7	2		30	6		78	7
	5	3		24	7		71	9
31	26	1		18	10		64	10
	21	2		16	11		57	11
	16	3		10	13		50	13
	11	5		7	15		43	14
	6	7	127	120	1		36	14
63	57	1		113	2		29	21
	51	2		106	3		22	23
	45	3		99	4		15	27
							8	31

3.2 Ranging Sequences Construction

The (frequency domain) cross-correlations among ranging sequences determine the BS receiver's capability to mitigate multiuser interference and control the false alarm probability. The detection probability depends largely on the autocorrelation [10]. It is desired that the cross-correlation values be as low as possible and the auto-correlation function behave like an Kronecker delta function. The latter ensures that the detection probability is insensitive to CFO. We present a sequence construction method with the above properties as the design criteria.

We first notice that an (n_c, k_c, t) BCH code has 2^{k_c} n_c -length codewords and can correct at least t errors. A t -error-correcting BCH code is chosen as a prototype due to the following properties:

- Property I: Both all-zero and all-one words are legitimate codewords.

Proof. If $u(X) = 0$, the codeword will be all-zero. $g(X)$ is a factor of $(X^{n_c} + 1)$ and $X^{n_c} + 1 = (X + 1)(X^{n_c-1} + X^{n_c-2} + \dots + X + 1)$. Based on Lemma (3.1.1),

$g(X)$ is a factor of $X^{n_c-1} + X^{n_c-2} + \dots + X + 1$ as well. Therefore all-one word is a legitimate codeword. \square

- Property II: Circular-shifted and/or complementary version of a given codeword remains a legitimate codeword.
- Property III: Except for the all-zero and all-one codewords, the codeword weight is lower-bounded by $2t + 1$ and upper-bounded by $n_c - (2t + 1)$, where n_c denotes the BCH codeword length.

Proof. The minimum distance of t -error-correcting BCH is $2t + 1$. Since the all-zero codeword is a legitimate codeword, the weight of other codeword will be larger than $(2t + 1)$. Similarly, the number of zero in one codeword are larger than $2t + 1$ except all-one codeword. \square

Thanks to fixed subcarrier numbers assigned for ranging, L_D , we choose the codeword length n_c as close to L_D as possible. An equivalent class (EC) is defined as a class, consists of a codeword and its all circular-shifted versions. Most EC size is n_c but there are some exceptions when n_c is not a prime number. In general, the candidate EC sizes are determined by zeros of the generator polynomial. However, if an EC size is less than 2α , where α is a small integer used as the design margin to allow certain fractional CFO uncertainty, then the corresponding EC shall be removed from further consideration as candidate sequences.

According to Properties I and II, all ECs can be partitioned into two groups such that if an EC belongs to a group then its complement EC must be in the other group. Because of the unknown channel impulse response and phase offset between the transmitter and the receiver, member sequences in one of the two groups shall be designated as prototype sequences and the other will be excluded from further consideration. When

the codewords are transmitted by BPSK signals, Property III implies that the cross-correlation value of any pair of BCH codeword will be in the interval $[-\frac{n_c-4t-2}{n_c}, \frac{n_c-4t-2}{n_c}]$. Thus one should select a t as large as possible to minimize the above correlation bound.

Since n_c cannot be arbitrary, the best one can do is to choose n_c as close to the required preamble length L_D as possible. For simplicity, we only consider the situation, $n_c \leq L_D$ but a similar approach can be applied to deal with the case $n_c > L_D$. When n_c is less than L_D , one needs to insert $(L_D - n_c)$ dummy bits in every BCH codeword to satisfy the preamble sequence length requirement.

Since Peak-to-average-power ratio (PAPR) is a key design concern of an OFDM system as it dominates the system's power efficiency, these dummy data bits can be used to reduce the PAPR values of the preamble sequences as well. It is important that a transmitted initial ranging signal has a lower PAPR, because it guarantees that signals transmitted by the RSSs in the cell edge can arrive at the BS with sufficient power strength. The inserted indexes, I , are identical for every codeword, and the elements of dummy data are limited in $\{+1, -1\}$ for reducing the storage needs. The dummy data for each BCH codeword can be determined by (3.3). In practice, transmitted signals of RSSs are continuous waveforms not discrete ones. Therefore, an over-sampling factor $U \geq 4$ is needed to ensure a negligible approximation error if the discrete PAPR analysis is to be used to approximate analog one. The modified BCH codeword $\mathbf{m}_i = \mathbf{P}_c \mathbf{c}_i + \mathbf{P}_v \mathbf{v}_i$, where \mathbf{P}_c and \mathbf{P}_v are the matrices mapping the original codeword and dummy data into corresponding subcarriers respectively. The dummy data \mathbf{v}_i can be obtained by solving

$$\mathbf{v}_i = \arg \min_{\tilde{\mathbf{v}}_i} \|\mathbf{Q}(\mathbf{P}_c \mathbf{c}_i + \mathbf{P}_v \tilde{\mathbf{v}}_i)\|_\infty \quad (3.3)$$

where \mathbf{Q} is the $UN \times L_D$ IDFT matrix, and $\tilde{\mathbf{v}}_i$ is the trial sequence [11]. After virtual sequence optimization, all we need to save are the information bits of \mathbf{c}_i and \mathbf{v}_i . Therefore, the needed bits can be reduced from L_D bits to $(L_D - n_c + k_c)$ bits.

If the linear range of high power amplifier (HPA) is not sufficient, the large PAPR leads to in-band distortion and out-of-band radiation. The lower PAPR value the ranging

sequence is, the higher priority it could be selected as a ranging sequence. However, to eliminate the ambiguity caused by carrier frequency offset, once a basic preamble sequence is selected, its right and left 2α circular-shifted versions (4α in total) within the EC must be removed from the candidacy of the ranging sequences. The remaining sequences are integer CFO-invariant. If the EC size is in the range, $(2\alpha + 1, 4\alpha + 1)$, only one basic sequence could be chosen.

The number of ICFO-invariant ranging sequences may not be able to meet the sequence family size or PAPR requirement. Tradeoffs among correlation values, PAPR, and number of legitimate sequences allow us to take one of the following two alternatives:

- Trade higher correlation value for a larger size of the ranging sequence family: Increase the message dimension k_c of the BCH code until the family size requirement is met.
- Trade higher correlation for a smaller PAPR: Puncture m_p bits from each prototype sequence (so that one has m_p more positions to allocate virtual bits) until the PAPR or other system requirements is met.

3.3 Multi-user Ranging Signal Detection and Timing Offset Estimation

The frequency domain ranging signal \mathbf{X}_i^R for the i th ranging user, R_i , is denoted by

$$\mathbf{X}_i^R(k) = \begin{cases} A_i \mathbf{c}_i, & k \in S_r \\ 0, & \text{otherwise,} \end{cases} \quad (3.4)$$

where $\mathbf{c}_i = [c_i(p)]_{p \in S_r} = [c_i(u_1), c_i(u_2), \dots, c_i(u_{L_D})]$, $u_v \in S_r$, A_i , S_r , and L_D are the ranging sequence used by R_i , its relative amplitude, the subcarrier set assigned for serving the ranging process, and the length of \mathbf{c}_i , which is the same as the cardinality of S_r , respectively. As an OFDMA system often allocates only a portion (L_D subcarriers) of the available spectrum for initial ranging, it is more convenient to design the ranging sequences in frequency domain instead of time domain. The maximum transmission

delay D_{max} (samples) equals to the sum of the maximum delay spread and the round-trip propagation delay between the BS and a RSS at the boundary of the cell. Furthermore, the maximum delay spread among all uplink ranging channels is L (samples). To avoid inter subcarrier interference (ICI) and inter symbol interference (ISI), the length of the cyclic prefix (CP), N_g , must be larger than D_{max} [9]. This assumption is not restrictive, since in many standardized OFDM systems the initialization blocks are usually preceded by long CPs. With the CP inserted, the time domain ranging signal for R_i is $\{x_i(n), n = -N_g, -N_g + 1, \dots, N\}$, where N is the FFT size.

Assuming the uplink channels remain static within a symbol duration and ignoring the presence of noise, we express the received ranging waveform $y_i^R(n)$ for R_i as

$$y_i^R(n) = \sum_{l=0}^{L-1} h_i(l)x_i(n-l) \quad (3.5)$$

where $h_i(l)$, $l = 0, \dots, L-1$ are the associated channel tap weights. The remaining $N - L_D$ subcarriers are assigned to N_{DSS} data subscriber stations (DSSs) which have already completed their initial ranging processes and are assumed to be perfectly synchronized with the BS' time and frequency scales. $y_i^D(n)$ denotes the signal of the i th DSS. The received signal at the BS thus becomes

$$y(n) = \sum_{i=0}^{N_{RSS}-1} y_i^R(n - d_i) e^{j2\pi\varepsilon_i n / N} + \sum_{i=0}^{N_{DSS}-1} y_i^D(n) + w(n)$$

where $\{w(n)\}$ are independent and identical distributed (i.i.d.) complex circular symmetric Gaussian random variables with mean zero and variance $\sigma_w^2 = E[|w(n)|^2]$ and d_i , ε_i represent the timing offset and normalized CFO of R_i .

The baseband receiver removes the CP and takes DFT on the remaining received samples of each frame. The L_D -dimensional vector \mathbf{Y} is obtained by stacking the components of the DFT output vector corresponding to the subcarriers assigned for the ranging process (i.e., $k \in S_r$). Since the DSSs are assumed to be perfectly synchronized,

their signals will not contribute to \mathbf{Y} ,

$$\mathbf{Y} = \sum_{i=0}^{N_{RSS}-1} A_i \mathbf{F}(\varepsilon_{ip}) \mathbf{H}_i \mathbf{c}_i + \mathbf{n}, \quad (3.6)$$

where $\mathbf{H}_i = \text{diag}(H_i(u_1), H_i(u_2), \dots, H_i(u_{L_D}))$ is a diagonal matrix with $(H_i(u_1), H_i(u_2), \dots, H_i(u_{L_D}))$ along its main diagonal, $H_i(u_v)$ is the channel gain on the u_v th subcarrier of the i th RSS, and \mathbf{n} is the L_D -dimensional AWGN vector. Furthermore, $\mathbf{F}(\varepsilon_i)$ is a $L_D \times L_D$ Toeplitz matrix whose a th row and the b th column entry is given by [9]

$$f_{u_a, u_b}(\varepsilon_i) = \frac{\sin(\pi(\Delta_{ba} + \varepsilon_i))}{N \sin(\pi(\Delta_{ba} + \varepsilon_i)/N)} e^{j\pi(\Delta_{ba} + \varepsilon_i)(N-1)/N}, \quad (3.7)$$

where $\Delta_{ba} = u_b - u_a$.

A RSS intending to start an initial ranging should first derive its initial frequency and timing estimates from a downlink control signal broadcasted by the BS. As the residual CFOs are due to Doppler shifts, oscillator instabilities and/or estimation errors it is reasonable to assume that they lie within a small fraction of a subcarrier spacing, i.e., $|\varepsilon_i| \approx 0$, and $\mathbf{F}(\varepsilon_i)$ in (3.6) can be replaced with \mathbf{I}_{L_D} , where \mathbf{I}_{L_D} is an identity matrix of order L_D . Note that \mathbf{Y} consists of possibly more than one ranging sequence. To decouple all possible active RSSs, \mathbf{Y} will be individually correlated with all ranging sequence candidates, the BS allows the RSS to choose one ranging sequence from the set and to transmit it back to the BS. The correlation is performed in the frequency domain and then transformed back to the time domain [5]. In other words, $\tilde{\mathbf{Y}}_i = [\tilde{Y}_i(k)]_{k \in S_r}$ is given by

$$\tilde{Y}_i(k) = \begin{cases} Y(k)c_i^*(k), & k \in S_r \\ 0, & \text{otherwise} \end{cases}$$

For the time-domain sample vector $\tilde{\mathbf{y}}_i = \text{IDFT}[\tilde{\mathbf{Y}}_i]$, if the desired signal \mathbf{c}_i is active, its contribution will be concentrated on a few (time) indices [5][13]. On the other hand, the interference from other ranging signals will be spread over all (time) indices. Therefore,

we first compute the sliding-window signal energy and average noise power estimates by

$$\xi_i(n) = \sum_{l=0}^{L-1} \tilde{y}_i^2(|(l+n)|_N), \quad (3.8)$$

$$\sigma_i^2 = \sum_{l=D_{max}+1}^N \frac{\tilde{y}_i(l)^2}{N - D_{max} - 1} \quad (3.9)$$

where $|\cdot|_N$ represents the modular N operation. Based on the above two estimates we obtain an estimate for the signal-to-interference-and-noise ratio (SINR), ζ_i , and that for the timing offset, \hat{d}_i , by

$$\zeta_i = \max_n \frac{\xi_i(n)}{\sigma_i^2} \quad (3.10)$$

$$\hat{d}_i = \arg \max_n \frac{\xi_i(n)}{\sigma_i^2} \quad (3.11)$$

If D_{max} is close to N , σ_i^2 is to be obtained by taking average of $\tilde{y}_i^2(l)$ over all time stamps l which not in the set $\{\hat{d}_i, \dots, \hat{d}_i + L\}$. A ranging sequence \mathbf{c}_i is declared present if $\zeta_i \geq \eta$, and is assumed to be absent if $\zeta_i < \eta$.

3.4 Simulation Result and Discussion

3.4.1 Simulation Setup

The OFDMA system parameters used in the simulations reported in this section are selected from [12] and [13]. The uplink bandwidth is 10 MHz, and the subcarrier spacing is 10.9375 KHz. The FFT size N is 1024. ITU vehicular A channel model is used and the sampling interval T_s is 89.285 ns. We consider a cell size of radius 5 km so that the maximum transmission delay $d_{max}=33.34 \mu s = 373$ samples. N_g is assumed to be 512 samples to satisfy the condition $N_g > d_{max}$. The subcarriers numbers used by ranging process are 72. The supported maximum speed of RSS is 120 Km/hr and carrier frequency is 2.5 GHz. The normalized residual CFOs of RSSs thus lie within the range $[-0.05, 0.05]$ and are assumed to be i.i.d. for different RSSs. Because our proposed algorithm utilizes the FFT output data, the interference mainly comes from RSSs in

same group. We assume there are K active RSSs in the group and each BS has its own 64 ranging sequences for one subband. Eight non-overlapping ranging sequence sets are proposed for system reuse. The characters of employed BCH, (n_c, k_c, t) , are $(63, 16, 11)$. The needed memory to save one ranging sequence are 25 bits and the compression ratio is 34.7 %. The RSS probably has a inaccurate frequency estimation, and its transmitted signal will be with a large frequency offset. Therefore, α is 15 to avoid the ranging sequence is declared as its circular shift version. Some or all of the following RSS distributions are considered: (i) $K = 1$, (ii) $K = 2$, (iii) $K = 4$, within one ranging time-slot.

3.4.2 PAPR Performance

The over-sampling factor U is 4 to ensure a negligible approximation error if the discrete PAPR analysis is to be used to approximate analog waveforms. The PAPRs of the proposed ranging sequences and the PRBS sequences are plotted in Fig 3.1. We can see that the PAPR values of BCH-based ranging sequences are about 2.7 dB lower than those of PRBS preambles on average. It can improve the efficiency of a power amplifier from 19.95% to 37.15%.

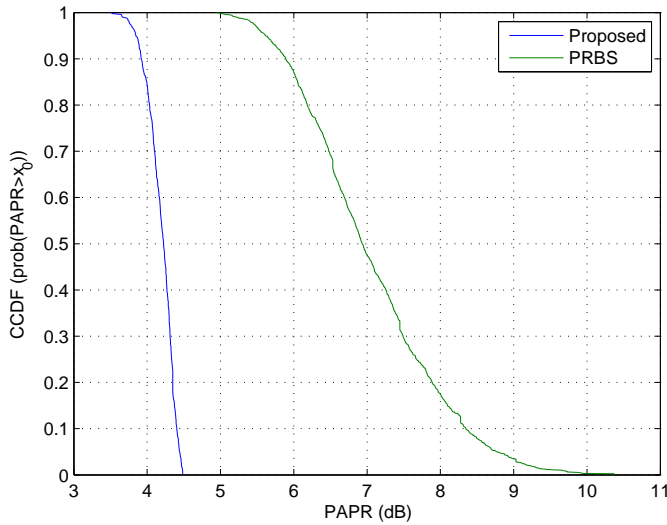


Figure 3.1: CCDF performance of proposed sequences and PRBS.

3.4.3 Multi-User Detection Performance

SNR is defined as the ratio of signal variance to noise variance in time domain. The threshold, η , is independent on K and SNR and is fixed at 9 dB. Comparisons are made with PRBS ranging schemes. The result of Fig. 3.2 indicates that the proposed scheme performs remarkably better than PRBS because of its lower correlations between any pairs in the same group. We can see that the fewer active RSS case has slightly higher false alarm, because noise plus the interference level in (3.9) is lower than one in more active RSSs case. It implies that $\xi_i(\hat{d}_i)$ be compared with relatively lower threshold, $\sigma_i^2\eta$. The lower false alarm probability benefits the system, because it prevents that the system wastes its resources on allocating the subbands to non-existing RSSs.

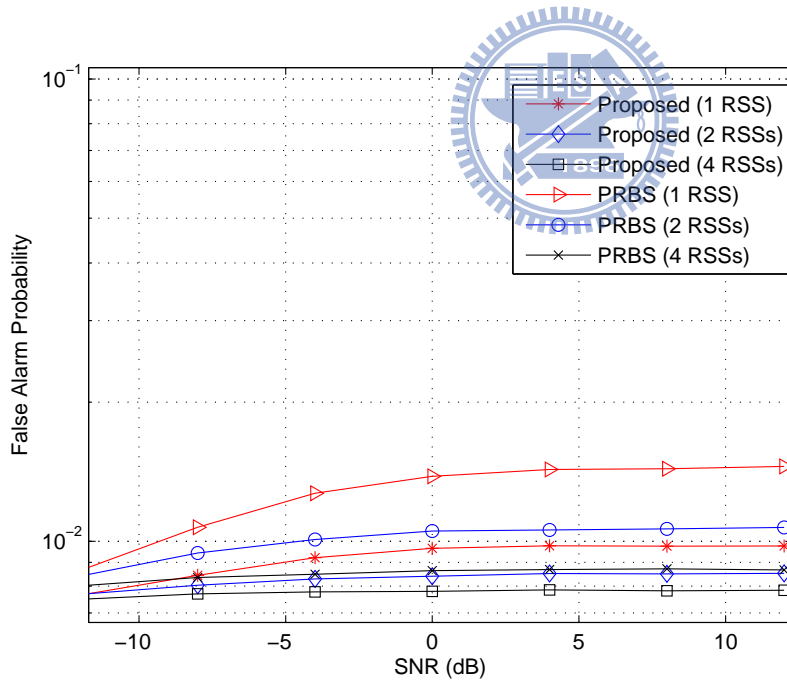


Figure 3.2: Probability of false alarm as a function of average SNR.

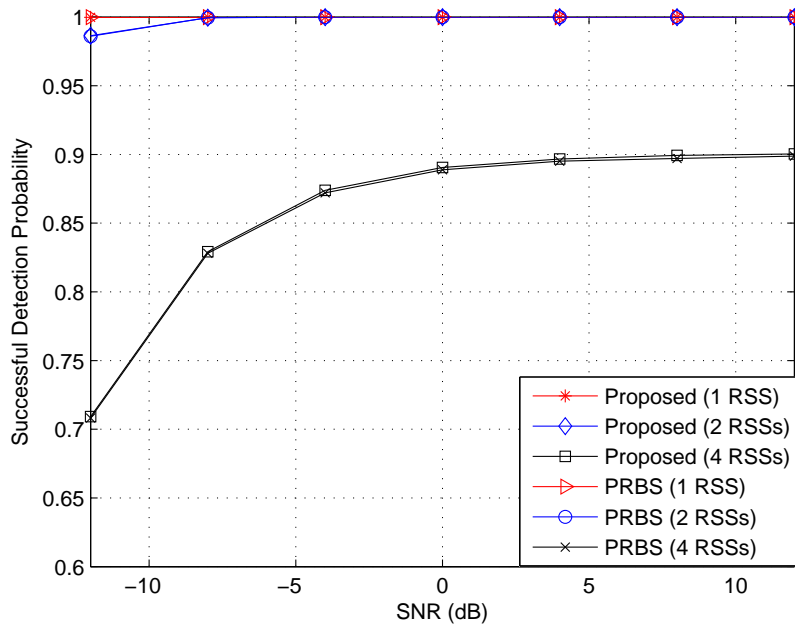


Figure 3.3: Detection probability performance as a function of average SNR.

Fig. 3.3 shows the probability of correct detection (P_D) performance versus the average SNR. The detection capability of our sequences is almost the same as that of PRBS. The main reason is that the time-domain autocorrelation of a ranging sequence does not depend on the corresponding codeword but on the channel assignment scheme, if the ranging sequence is MPSK modulated. The power spectrum densities are identical if the ranging sequences are MPSK modulated with the same predefined channel assignment. For $K = 4$, since η is fixed, the signal energy estimate $\xi_i(\hat{d}_i)$ has to exceed a larger $\sigma_i^2\eta$, the detection probability decreases. However, even for this case it is still close to 90% when SNR is greater than 4 dB.

3.4.4 Performance of Timing Estimator

Fig. 3.4 plots the root mean squared timing offset estimation error, as a function of the average SNR for the various RSS distributions. In each realization, the true transmission delays are taken randomly from the interval $[0, d_{max}]$. Although, the accuracy of timing estimation depends mostly on its autocorrelation function, a lower

cross-correlation can still improve the accuracy when there are 4 active RSSs. After each RSS has successfully finished initial ranging and adjusted its timing offset, the BS will be able to support more RSSs in one group for subsequent periodic ranging since most of the round-trip delay uncertainty has been removed and the CP length can be reduced accordingly.

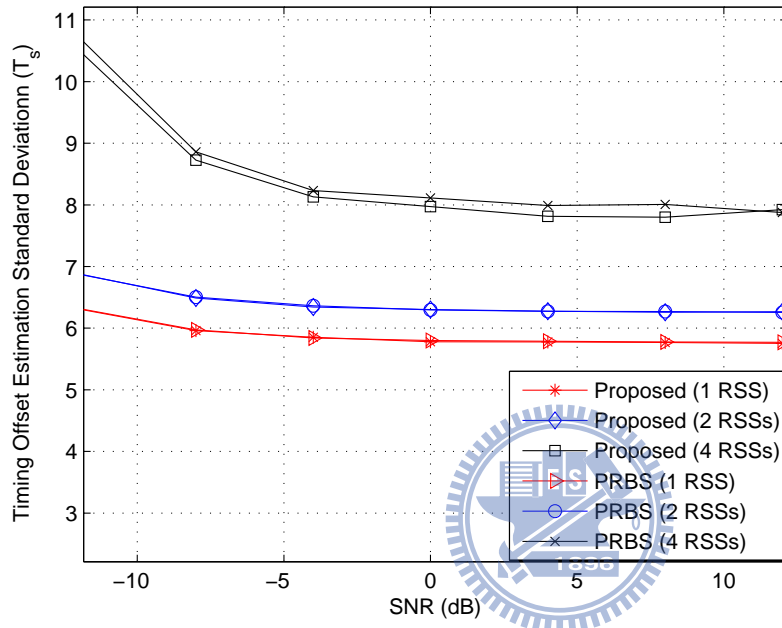


Figure 3.4: Timing jitter behavior as a function of the average SNR.

Chapter 4

Two-step UL Synchronization for Pico/Femtocells

4.1 Overlaid Network

Picocell and Femtocell deployment is an important feature in the next generation (4G) wireless mobile communication systems, such as WiMAX 2.0 systems defined by IEEE 802.16m and LTE-Advanced systems defined by 3GPP Release 10. As shown in Fig. 4.1, cellular OFDM communication system comprises a macro/micro base station BS, pico/femto base stations (BS), and mobile stations (MS). The pico/femto base stations have smaller cell coverage, while the overlaying macro/micro base station which has much larger cell coverage. The deployment of femto-BSs benefits both users and service providers. Subscribers accessing femto-BSs can achieve greater signal strength and better quality of service because of the short transmit/receive distance. In addition, the short-range and low-power properties of femto-BSs enable more subscribers to use the same pool of radio resources by accessing different femto-BSs in different areas. This also benefits service providers from increasing system capacity and spectral efficiency. The data traffic can be offloaded via femtocells and it is one popular solution to Network congestion. In addition, the operational cost of service providers is greatly reduced since femto-BSs are paid for and maintained by subscribers.

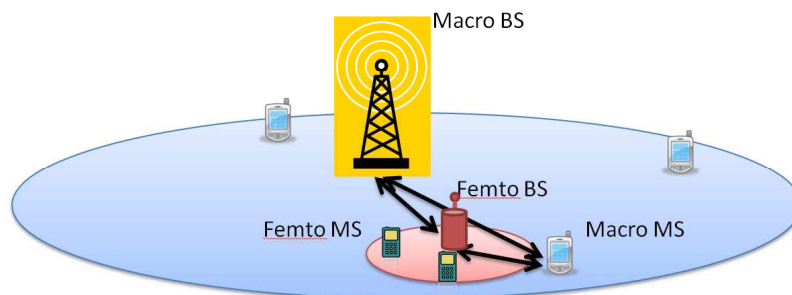


Figure 4.1: Illustration to a hierarchical cell structure of macro/microcells and pico/femtocells in a cellular OFDM communication system

4.2 UL Network Timing Synchronization

Network timing synchronization becomes an important issue when pico/femtocells are deployed together with overlaying macro/microcells, especially in a co-channel development scenario. Network timing offset will destroy the orthogonality of OFDM symbol and lead to severe interference cross whole operating frequency band such that any resource planning fails. Network timing synchronization is essential and has to be kept so that radio signals from a pico/femto base station and an overlaying macro/micro base station over the air do not interfere with each other.

TDD OFDM comprises DL subframes, UL subframes and transmission time gaps. Macro station transmits data during DL subframes and receives data during UL subframes. Each DL subframe is followed by an UL subframe after a predefined transmit transition gap (TTG) time, and each UL subframe is followed by a DL subframe after

a predefined receive transition gap (RTG) time. TTG is always larger than or equal to RTG.

Pico/femto base station is synchronized with overlaying macro, and has approximately the same DL and UL transmission timing due to its physical proximity with BS. For mobile station that is served by macro, it receives data during DL subframes and transmits data during UL subframes. After DL and UL synchronization with its serving BS, each DL subframe of MS synchronizes with each DL subframe of BS with a DL propagation delay, while each UL subframe of MS synchronizes with each UL subframe of BS with an UL timing advance. However, the Pico/femto BS can not directly synchronize with the local time of macro station. In Fig. 4.2, the femto/pico has to postpone its DL transmission due to DL propagation delay. Similarly, the UL subframes of femtocells are advanced. If not doing so, the femtocells will cause cross-tier interference to nearby macro users in DL subframes and UL subframes of femtocells will be interfered by macro users.

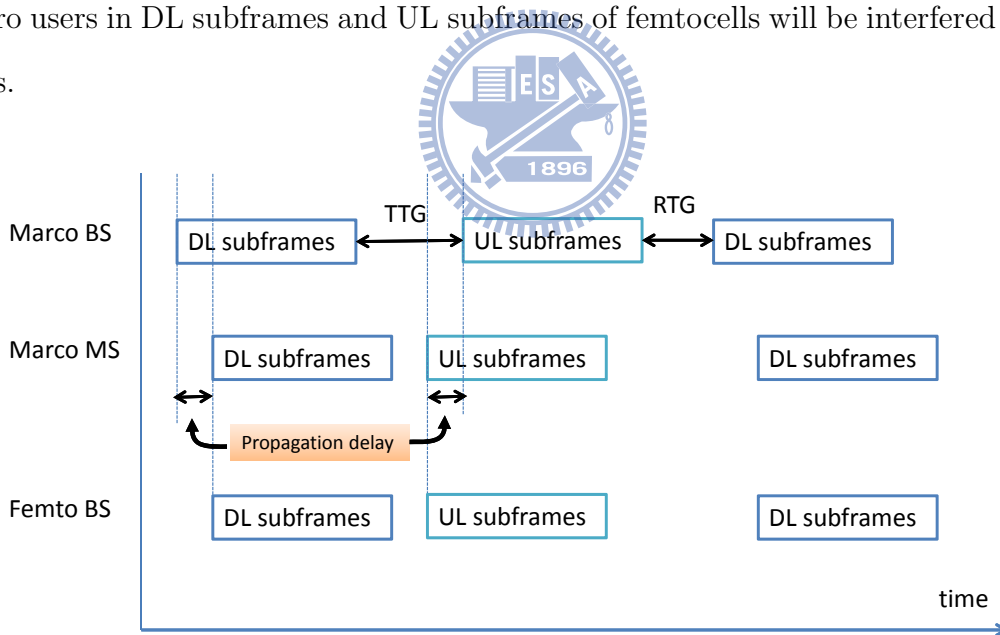


Figure 4.2: DL and UL subframes and transmission timing in cellular OFDM communication system

The problem is not fully solved. As illustrated in Fig. 4.2, the pre-defined TTG reserved to avoid the collision of downlink and uplink transmission may need to be adjusted

base on the deployment location of the pico/femto base station. However, for mobile stations which handover to a pico/femto cell or camping on in a pico/femtocell, there is no mechanism for them to know whether TTG adjustment is applied in the pico/femtocell. Without knowing this adjustment value, there will be different understandings about the uplink transmission timing between the mobile stations and the pico/femto BS. As illustrated in Fig. 4.3, the TTG adjustment causes the timing misalignment. The issue longer timing offset can be solved by extending CP. This solution, however, is associated with a few disadvantages. First, it requires a non-synchronous ranging channel to have a different CP length from a data channel in the same communication system. Second, the different CP lengths between non-synchronous ranging channel and data channel may result in interference with each other. Fatally, a non-synchronous ranging channel may have a different physical structure and code sequences than those of a synchronous ranging channel. Thus, without utilizing a unified synchronous ranging channel, hardware complexity and cost of a pico/femto BS may not be reduced. Although the distance between a fMs and a fBS is limited, but the information of TTG adjustment is not available at fMSs such that the time alignment at fBS will fail.

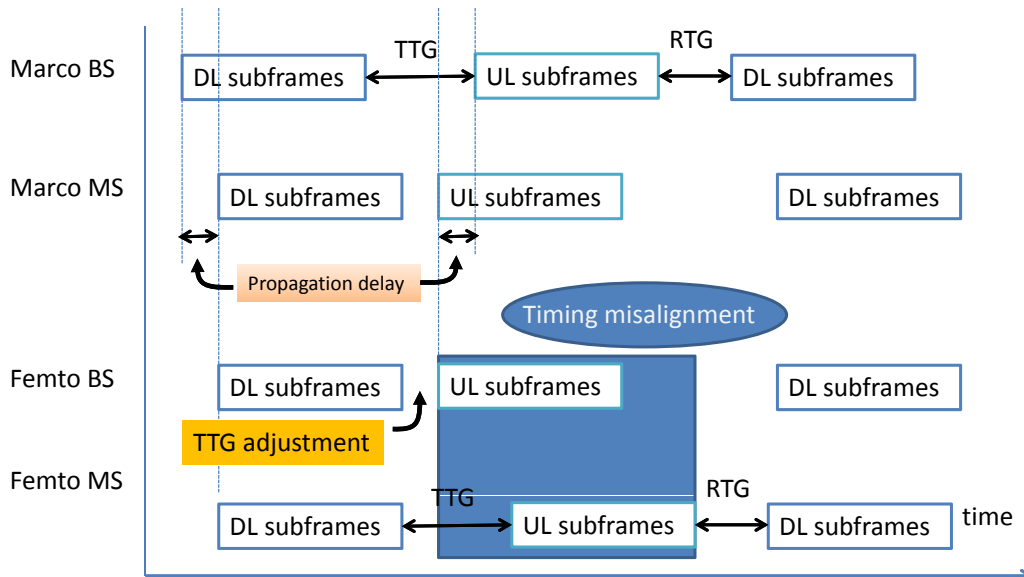


Figure 4.3: Timing misalignment is caused by TTG adjustment.

Specially, in IEEE 802.16m-D4 [14], the Padded Zadoff-Chu codes with cyclic shifts are used for the ranging preamble codes. The details of padded Zadoff-Chu sequences are described as follows. The p^{th} ranging preamble code $x_p\{n, k\}$ for the n th OFDMA symbol within a basic unit is defined by

$$x_p\{n, k\} = \exp\left\{-j\pi\left(\frac{r_p(n * 71 + k)(n * 71 + k + 1)}{211} + \frac{2 * k * s_p * N_{TCS}}{N_{FFT}}\right)\right\}, \quad (4.1)$$

$$k = 0, 1, \dots, N_{RP} - 1; n = 0, 1, 2$$

where

- p is the index for p^{th} ranging preamble code within a basis unit which is made as the s_p^{th} cyclic shifted sequence from the root index r_p of Zadoff-Chu sequence.
- $r_p = \text{mod}((1 - 2\text{mod}(\text{floor}(P/M), 2)) * (\text{floor}(p/(2M_s)) + r_{s0}) + 211, 211)$
- $p = 0, 1, \dots, N_{cont} - 1, \dots, N_{cont} + N_{dedi} - 1$
- $s_p = \text{mode}(p, M_s), p = 0, 1, \dots, N_{cont} + N_{dedi} - 1$
- The start root index r_{s0} is broadcasted.
- M_s is the number of cyclic shift per ZC root index and defined by $M_s = 1/G$.
- N_{TCS} is the unit of time domain cyclic shift per OFDMA symbol according to the CP length and defined by $N_{TCS} = N_{FFT}$
- G and N_{FFT} are the CP ratio and FFT size respectively.
- N_{RP} is the length of ranging preamble code per OFDMA symbol, i.e., $N_{RP} = 72$.

Originally, the padded Zadoff-Chu code are not suitable for asynchronous MSs due to the asynchronous MSs have wide-range timing offsets. The wide-range timing offset caused by TTG adjustment is not expected and leads to severe false detection probability of padded Zadoff-Chu sequence. To solve the issue, an amendment is proposed. In our

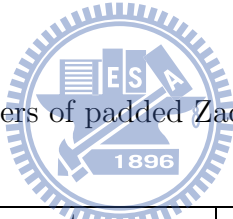
approach, the TTG adjustment information is quantized and broadcasted via broadcast channel. With the assisted information, the padded Zaddoff-Chu sequences can be used for femto MSs without causing any further side effects.

4.3 simulation result and discussion

4.3.1 Simulation Setup

The OFDMA system parameters used in the simulations reported in this section are selected from [12] and [13]. The uplink bandwidth is 10 MHz, and the subcarrier spacing is 10.9375 KHz. The FFT size is 1024. ITU vehicular A channel model and AWGN channel are considered. The subcarriers numbers used by ranging process are 72 and carrier frequency is 2.5 GHz. The operating SNR is 30 dB and the MAP is the chosen detection algorithm . The parameters of padded Zaddoff-Chu code as listed as follows:

Table 4.1: Parameters of padded Zaddoff-Chu sequences



parameter	values
The starting index (r_{so})	10
(N_{IN}, N_{HO}, H_{PE})	(16,16,16)
CP ratio (G)	1/8

4.3.2 Simulation result

In Fig. 4.4, it shows that the false detection probability of padded Zaddoff-chu code are not acceptable due to the timing offset caused by TTG adjustment. In our proposal, the 3-bit TTG adjustment information carried by broadcast channel can mitigate the false detection probability in AWGN case. In time dispersive channel, however, 3-bit TTG adjustment information is insufficient and 4-bit TTG adjustment information is adequate.

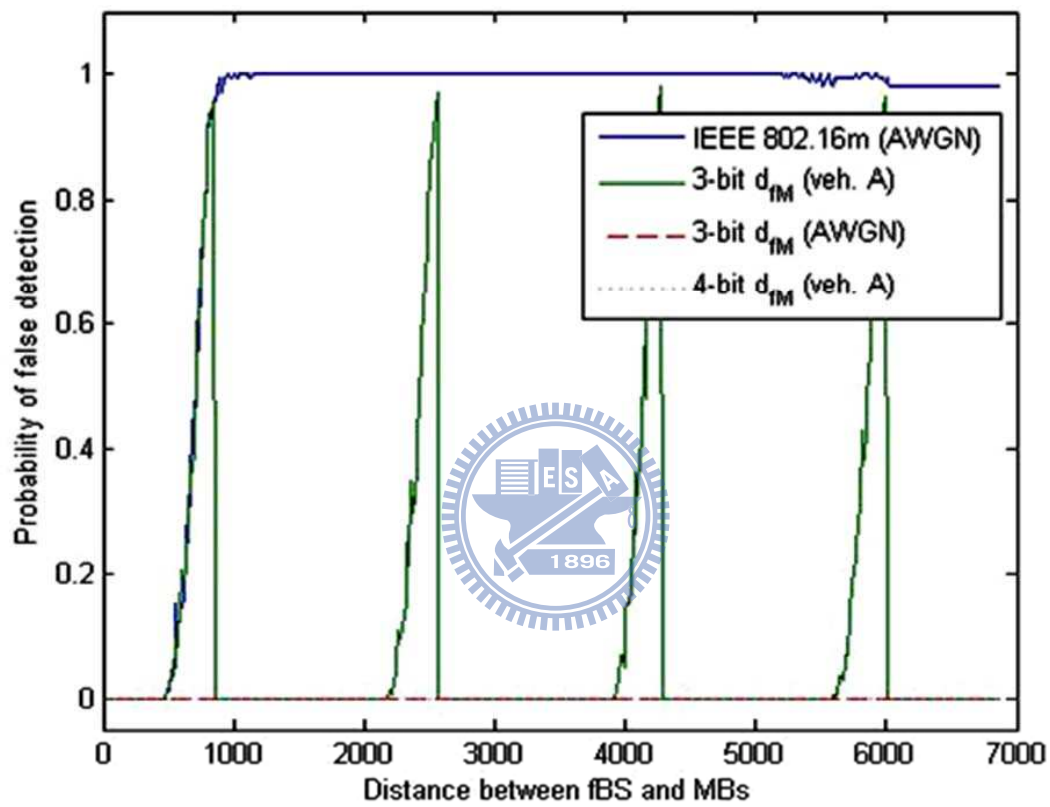


Figure 4.4: The false detection probability as a function of distance between fBS and mBS.

Chapter 5

Conclusion

A single OFDMA symbol based ranging signal design for initial ranging in a wireless mobile OFDMA system is proposed. Our proposed ranging signal design can be treated as a resource efficient approach. A ranging scheme that provides accurate multiple RSS' timing estimate is presented as well. Our approach is based on the idea of projecting the received multiple ranging signals onto the null (noise) space. No information about the active RSSs' strengths are needed in our proposal. Numerical results have demonstrated that the proposed solution is capable of offering excellent detection and false alarm probabilities performance and provides a good timing estimate for multiple active RSSs.

Besides, a novel BCH code based ranging signal design approach for ranging application in a wireless mobile OFDMA system is proposed. The ranging sequence family offers lower PAPR values and cross-correlations. Dummy data are inserted in reserved tones to render much improved PAPR performance. Our proposed sequences can be compressed and reconstructed with simpler implementation as well. Numerical results indicate that for a given detection probability, the proposed solution is indeed capable of offering improved false alarm probability performance and lower PAPR values.

Based on the knowledge from designing ranging sequences, we propose a two-step uplink synchronization for pico/femtocells. First, the pico/femtocells perform timing synchronization to the DL timing of the serving macrocell. The assisted information is carried via broadcast channel to announce the timing advance value of pico/femtocell.

The femto user will follow the instruction and adjust its uplink timing to prevent from interference. Simulation results show our timing advance signal can reduce the false detection probability of ranging sequences.



Bibliography

- [1] S. Lin, D. J. Costello, Error control coding: fundamentals and applications, Prentice Hall, 1983.
- [2] IEEE LAN/MAN Standard Committee, "Air interface for fixed and mobile broadband wireless access systems," IEEE 802.16e-2005.
- [3] J. Krinock, *et al.*, "Comments on OFDMA ranging scheme described in IEEE 802.16ab01/01r1," document IEEE 802.abs-01/24.
- [4] E. Dahlman , S. Parkvall , J. Skold , P. Beming, 3G Evolution, Second Edition: HSPA and LTE for Mobile Broadband, Academic Press, 2008.
- [5] X. Zhuang, *et al.* "Ranging improvement for 802.16e OFDMA PHY," document IEEE 802.16e-04/143r1.
- [6] X. Fu, Y. Li, and H. Minn, "A new ranging method for OFDMA systems," *IEEE Trans. Wireless Commun.*, vol. 6, no. 2, pp. 659 - 669, February 2007.
- [7] L. Sanguinetti, *et al.*, "An improved scheme for initial ranging in OFDMA-based Networks ," in *Proc., ICC*, Beijing, China, pp. 3469 - 3474, May 2008.
- [8] R. O. Schmidt, "Multiple emitter location and signal parameter estimation," in *Proc. RADC spectral Estimation Workshop*, 1979, pp. 243 - 258.

- [9] M. Morelli, C.-C. Jay Kuo, and M. O. Pun, "Synchronization techniques for orthogonal frequency division multiple access (OFDMA): A tutorial review," *Proceedings of the IEEE*, vol. 95, no. 7, pp. 1394 - 1427, July 2007.
- [10] C.-Y. Chen, Y.-J. Min, K.-Y. Lu, and C.-C. Chao, "Cell search for cell-based OFDM systems using quasi complete complementary codes," in *Proc. IEEE ICC*, pp. 4840 - 4844, Busan, Korea, Aug. 2006.
- [11] J. Tellado and J. M. Cioffi, "PAR Reduction in multicarrier transmission systems," *ANSI Document, T1E1.4 Technical Subcommittee*, 2008.
- [12] IEEE 802.16 Broadband Wireless Access Working Group, "Draft IEEE 802.16m evaluation methodology," IEEE 802.16m-07/037r1.
- [13] IEEE 802.16 Broadband Wireless Access Working Group, "IEEE 802.16m amendment working document (AWD)," IEEE 802.16m-09/0010r2 , June 2009.
- [14] IEEE LAN/MAN Standard Committee, "Air interface for fixed and mobile broadband wireless access systems," IEEE P802.16m/D4, February 2010.
- [15] K.-C. Lin and Y. T. Su, "Ranging signal design and its detection for OFDMA systems," in *Proc., ICASSP*, Taipei, Taiwan, pp. 2601 - 2604, April 2009.
- [16] K.-C. Lin and Y. T. Su, "Ranging sequences design for OFDMA systems," in *Proc., ICC*, Cape Town, South Africa, pp.1-5, May 2010.
- [17] P.-K. Liao, Y.-S. Lin, K.-C. Lin and Y. T. Su, "Two-Step uplink synchronization for pico/femtocell," 2011 U.S. Patent 0171949.

Curriculum Vitae

Personal Data								
Name	Chinese: 林坤昌 English: Kuhn-Chang Lin	Birthday		03 /FEB./1984				
Education								
Degree	Name of School	From		To		Major Subject	Graduated	
		Y	M	Y	M		Yes	No
Bachelor	National Chiao Tung University	2002	9	2006	6	Department of Communication Engineering	V	
Master.	National Chiao Tung University	2006	9	2011	11	Department of Communication Engineering		
Graduate Course:								
Digital Communication Information Theory Digital Signal Processing Matrix Computations Random Processes Coding Theory Estimation and Detection Queuing Theory Digital Receiver Technology Adaptive Signal Processing Optimization Theory and Application Machine Learning								
Publication:								
Conference Paper:								
K.-C. Lin and Y. T. Su, "Ranging Signal Design and its Detection for OFDMA Systems," <i>IEEE ICASSP2009</i> , Taipei, Taiwan, pp. 2601 – 2604, April 2009.								
Y.-C. Liu, K.-C. Lin and Y. T. Su, "Initial Synchronization for Multi-Cell OFDMA Systems," <i>IEEE ICC2009</i> , Dresden, German, pp. 1 – 5, June 2009								
Y.-H. Tung, K.-C. Lin and Y. T. Su, "A Linear Programming Approach for PAPR Reduction in OFDM Systems," <i>IEEE PIMRC</i> , Tokyo, Japan, Sep. 2009								
K.-C. Lin and Y. T. Su, "Ranging Sequences Design for OFDMA Systems," <i>IEEE ICC2010</i> , Cape Town, South Africa, pp. 1-5, May, 2010								

IEEE 802.16m Technical Contribution:

IEEE C802.16m-08_329r1, ``Ranging Code Design for IEEE 802.16m.”

IEEE C802.16m, System Description Document (SDD), ``Ranging code design consideration for IEEE 802.16m.”

IEEE C802.16mUL_ctrl-08/024r1, ``UL Ranging Design Consideration for IEEE 802.16m.”

IEEE C802.16m-10/0220, ``Uplink Timing Advance Broadcasting for Ranging in Femtocell for IEEE 802.16m.”

Cosigned Contribution:

IEEE C802.16m-UL_PHY_Ctrl_08/044r1, ``Harmonized SDD Text on Ranging Channel Structure for Non-Synchronized MSs.”

C80216mUL_ctrl-08_015.doc, ``Proposed Text for Intermediate Draft of Uplink Control Structure in SDD.”

LTE-A Technical contributions:

R2-105452, ``Investigation on Applying DRX Mechanism for In-Device Coexistence.”

R2-106348, ``Gap Analysis for LTE-WiFi Coexistence by Legacy Solutions.”

R2-110255, ``Analysis in TDM Solution for WiFi Coexistence.”

R2-114201, `` Evaluation on DRX based TDM Solution.”

US patent:

P.-K. Liao, Y.-S. Lin, K.-C. Lin and Y. T. Su, ``Two-Step Uplink Synchronization for Pico/Femtocell," 2011 U.S. Patent 0171949.

I.-K. Fu, K.-C. Lin and Y. T. Su, `` Method of TDM In-Device Coexistence Interference Avoidance," is submitted